Transcription factors FOXA1 and FOXA2 maintain dopaminergic neuronal properties and control feeding behavior in adult mice

Alessandro Pristerà[a], Wei Lin[a], Anna-Kristin Kaufmann[b], Katherine R. Brimblecombe[c], Sarah Threlfell[c,d], Paul D. Dodson[b,d], Peter J. Magill[b,d], Cathy Fernandes[e], Stephanie J. Cragg[c,d], and Siew-Lan Ang[a,1]

[a]The Francis Crick Institute Mill Hill Laboratory, London NW7 1AA, United Kingdom; [b]Medical Research Council Brain Network Dynamics Unit, Department of Pharmacology, University of Oxford, Oxford OX1 3TH, United Kingdom; [c]Department of Physiology, Anatomy and Genetics, University of Oxford, Oxford OX1 3QX, United Kingdom; [d]Oxford Parkinson's Disease Centre, University of Oxford, Oxford OX1 3PT, United Kingdom; and [e]Social, Genetic and Developmental Psychiatry Centre, Institute of Psychiatry, Psychology and Neuroscience, King's College London, London SE5 8AF, United Kingdom

Edited by Richard D. Palmiter, University of Washington, Seattle, WA, and approved July 8, 2015 (received for review February 26, 2015)

Midbrain dopaminergic (mDA) neurons are implicated in cognitive functions, neuropsychiatric disorders, and pathological conditions; hence understanding genes regulating their homeostasis has medical relevance. Transcription factors FOXA1 and FOXA2 (FOXA1/2) are key determinants of mDA neuronal identity during development, but their roles in adult mDA neurons are unknown. We used a conditional knockout strategy to specifically ablate FOXA1/2 in mDA neurons of adult mice. We show that deletion of *Foxa1/2* results in down-regulation of tyrosine hydroxylase, the rate-limiting enzyme of dopamine (DA) biosynthesis, specifically in dopaminergic neurons of the substantia nigra pars compacta (SNc). In addition, DA synthesis and striatal DA transmission were reduced after *Foxa1/2* deletion. Furthermore, the burst-firing activity characteristic of SNc mDA neurons was drastically reduced in the absence of FOXA1/2. These molecular and functional alterations lead to a severe feeding deficit in adult *Foxa1/2* mutant mice, independently of motor control, which could be rescued by L-DOPA treatment. FOXA1/2 therefore control the maintenance of molecular and physiological properties of SNc mDA neurons and impact on feeding behavior in adult mice.

FOXA1 | FOXA2 | dopamine | burst firing | feeding

Most dopaminergic (DAergic) neurons in the adult midbrain are grouped in the ventral tegmental area (VTA) and substantia nigra pars compacta (SNc). VTA and SNc neurons have been classically linked to diverse functions and different projection targets (1). VTA neurons project to the ventral striatum, cortical areas, and limbic structures. Midbrain dopaminergic (mDA) neurons in this group are implicated in emotional behavior, motivational functions, and reward mechanisms (2–4). On the other hand, SNc neurons mainly project to the dorsal striatum and regulate motor function (5). mDA neurons are of major interest in biomedical research because degeneration of SNc mDA neurons is the hallmark of Parkinson's disease (6). In addition, mDA neuron dysfunction is associated with cognitive impairment, motivational deficits, addiction, and drug abuse (7–10). The identification of factors that maintain dopamine (DA) function in developed adult neurons may contribute to the understanding of the mechanisms supporting the homeostasis of mDA neurons and therefore help in identifying therapeutic targets to treat disorders arising from dysfunctional mDA neurons.

FOXA1 and FOXA2 (FOXA1/2) are members of the winged-helix/forkhead transcription factors, which share over 95% homology between mice and humans (11). FOXA1/2 are so-called "pioneer proteins" that, by binding to tightly condensed chromatin in promoters and enhancer regions, facilitate access of other transcription factors (12, 13). FOXA1/2 regulate the development of diverse organs, including the lung, liver, pancreas, prostate, and kidneys (14). We have also found that FOXA1/2 play a crucial role in the generation of mDA neurons during early and late development, regulating both their specification and differentiation in a dose-dependent manner (15). FOXA1/2 operate in successive feedforward loops with different cofactors to regulate the expression of distinct target genes in neuronal progenitors and immature neurons (16–19). There is accumulating evidence that transcription factors regulating the specification and differentiation of mDA neurons retain expression in the adult brain (20). Recent papers have addressed the adult-specific role of some of these transcription factors. For example, OTX2 expression is restricted to the VTA in adult mDA neurons and is necessary to control VTA identity and to protect these neurons from 1-methyl-4-phenyl-1,2,3,6-tetrahydropyridine (MPTP)-mediated toxic insults (21). In addition, NURR1 has recently been found to sustain nuclear-encoded mitochondrial gene expression and to preserve neurite integrity of adult mDA neurons (22). A recent study from our laboratory demonstrated that late developmental inactivation of FOXA1/2 in mDA neurons leads to a phenotypic change, and mDA neurons lose their DAergic markers without incurring cell loss (23). FOXA1/2 are also expressed in adult mDA neurons (23, 24), but their role in these neurons has not been resolved. *Foxa2* heterozygous mice carrying a null allele of *Foxa2* show late-onset degeneration of mDA neurons at 18 months of age, which may be due to defects in either developmental or adult functions (24).

In this report, we determined the role of FOXA1/2 in adult mDA neurons using a conditional (drug-inducible) recombinase-based

Significance

Dopaminergic neurons in the brain control voluntary movement and a variety of cognitive functions, including reward–motivation mechanisms, mood regulation, addiction, and memory. Understanding how dopaminergic neurons' phenotype and function are maintained throughout their life span is of great importance in the light of the diverse roles that they play. Transcription factors FOXA1/2 control dopaminergic neurons' development and then retain their expression in adult neurons. The role of these factors during development is well established, but the meaning of their expression in the adult is still not well understood. We demonstrate here that FOXA1/2 are crucial to maintain key cellular and functional features of dopaminergic neurons in the adult brain. We also show that FOXA1/2-mediated deficits ultimately affect feeding behavior.

Author contributions: A.P., W.L., A.-K.K., S.T., P.D.D., P.J.M., C.F., S.J.C., and S.-L.A. designed research; A.P., W.L., A.-K.K., K.R.B., S.T., and C.F. performed research; A.P., W.L., A.-K.K., S.T., P.D.D., P.J.M., C.F., S.J.C., and S.-L.A. analyzed data; and A.P., A.-K.K., S.T., P.D.D., P.J.M., C.F., S.J.C., and S.-L.A. wrote the paper.

The authors declare no conflict of interest.

This article is a PNAS Direct Submission.

[1]To whom correspondence should be addressed. Email: siew-lan.ang@crick.ac.uk.

This article contains supporting information online at www.pnas.org/lookup/suppl/doi:10.1073/pnas.1503911112/-/DCSupplemental.

strategy for gene deletion (CreERT2-*loxP*). We show that FOXA1/2 are necessary for maintaining normal DA synthesis and transmission, as well as burst-firing activity in SNc neurons in adult mice. Interestingly, deletion of FOXA1/2 in adult mDA neurons leads to a feeding behavior deficit and lethality in affected mice, which is not accompanied by an overall hypoactivity.

Results

FOXA1/2 Are Expressed in mDA Neurons in the Adult Brain and Can Be Efficiently Deleted in *Slc6a3*$^{CreERT2/+}$;*Foxa1/2*$^{flox/flox}$ Mice. In agreement with a previous report from our laboratory (23), we found that FOXA1/2 are expressed in the vast majority of tyrosine hydroxylase (TH)-positive mDA neurons of the VTA and SNc (Fig. 1 *A*–*C*) of adult *Foxa1/2*$^{flox/flox}$ mice, hereafter referred to as control mice. Sporadic TH-negative neurons within the midbrain, expressing FOXA1/2 were also detected (Fig. 1*B*, dotted arrows, left panel). Immunoreactivity for FOXA1/2 was localized to the nuclei of neurons (Fig. 1*B*, arrows), consistent with the DNA binding properties of FOXA1/2. To induce the deletion of FOXA1/2 specifically in mDA neurons, we administered tamoxifen intraperitoneally to *Slc6a3*$^{CreERT2/+}$;*Foxa1/2*$^{flox/flox}$ adult mice. In these tamoxifen-treated animals, henceforth referred to as adult *Foxa1/2* conditional knockout (cKO) mice, we observed a very efficient gene deletion, as demonstrated by the lack of FOXA1/2 immunoreactivity in the vast majority of mDA neurons (Fig. 1 *A*–*C*), whereas their expression is not affected in TH-negative cells (Fig. 1*B*, dotted arrow right panel). Quantification of the deletion is shown in Fig. 1*C*. These results indicate that FOXA1/2 expression is maintained into adulthood in the vast majority of mDA neurons, and that tamoxifen-induced Cre activity in DA transporter (DAT)-expressing neurons represents an efficient strategy to achieve robust knockdown of FOXA1/2 in adult mDA neurons.

DAT is also expressed in some cells in the hypothalamus and olfactory bulbs (Paul Allen Brain Atlas; www.brain-map.org). Therefore, to further assess the specificity of our model, we analyzed FOXA1/2 immunoreactivity in the hypothalamus and olfactory bulbs of control mice, and identified DAergic cells by DAT expression. We found strong FOXA1/2 immunoreactivity in the mDA population (Fig. S1*A* and Fig. 1) and colocalization of FOXA1/2 and DAT expression in this DAergic neuronal population (Fig. S1*A*). In contrast, we did not observe coexpression of DAT with FOXA1/2 in other DAergic nuclei (Fig. S1), designated A12, A13, A14, and A15 groups in the hypothalamus, and A16 group in the olfactory bulb (25). DAergic neurons are also present in the enteric nervous system (26). FOXA1/2 are not expressed in enteric neurons, identified by expression of the panneuronal marker PGP9.5 (27), in the myenteric ganglia (Fig. S1*B*). Altogether, these data demonstrate that our mouse model specifically addresses the role of FOXA1/2 in mDA neurons.

FOXA1/2 Positively Regulate DA-Specific Phenotype and DA Content in Adult Neurons. Previous studies have demonstrated roles for FOXA1/2 in initiating and maintaining the molecular identity of mDA neurons during development at the transcriptional level (15–19). We therefore determined whether FOXA1/2 are still required to maintain the expression of transcripts that are pivotal for mDA neuron function, such as mRNA of *Th*, *Ddc*, *Slc18a2*, *Slc6a3*, and *Drd2* genes, by real-time quantitative PCR (rt-qPCR). RNA was isolated from laser-captured midbrain tissue containing the SNc and VTA. Statistically significant decreases in *Th*, *Ddc*, *Slc18a2*, *Slc6a3*, and *Drd2* transcripts were observed in adult *Foxa1/2* cKO mice, compared with levels in control mice, after 1 week as well as 6 weeks post-tamoxifen treatment (Fig. 2*A*). These data demonstrate that FOXA1/2 are still required to maintain the expression of DA neurotransmitter identity genes in adult mDA neurons.

TH is the enzyme that catalyses the rate-limiting step in DA synthesis, and we explored whether a change in *Th* transcript was

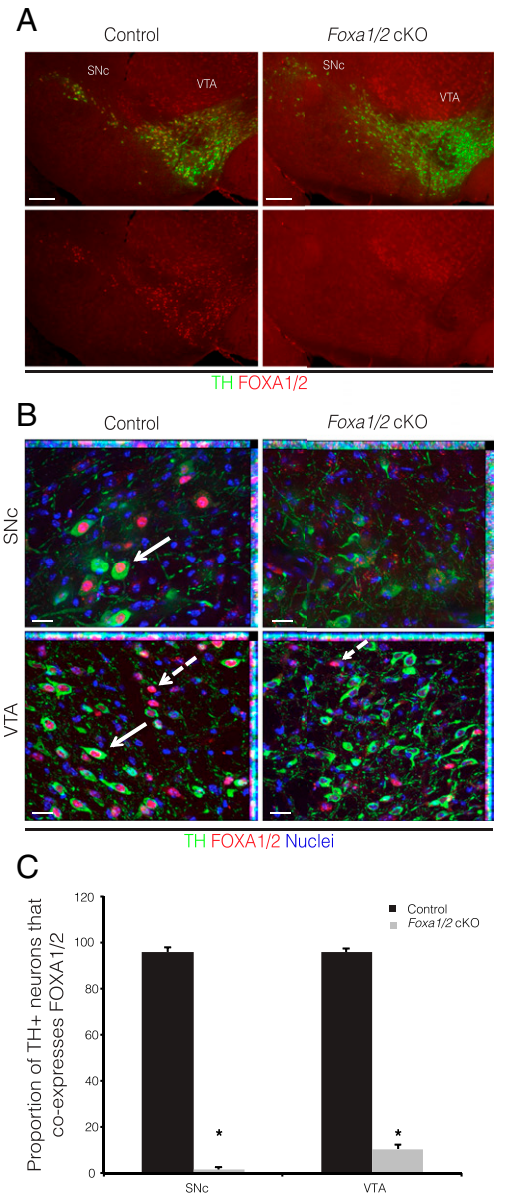

Fig. 1. FOXA1/2 are expressed in adult mDA neurons and can be efficiently deleted following CreERT2-mediated recombination. Low-magnification images show the distribution of FOXA1/2 immunoreactivity in mDA neurons of control mice, and their absence in adult *Foxa1/2* cKO mice. VTA and SNc neurons are identified by TH staining. [Scale bars: 200 μm (*A*).] Representative maximum-intensity projection images of FOXA1/2 immunoreactivity within the VTA and SNc of control and adult *Foxa1/2* cKO mice are shown in *B*. Solid arrows indicate TH+/FOXA1/2+ neurons, and dotted arrows indicate TH–/FOXA1/2+ cells. (Scale bars: 20 μm.) Quantification of FOXA1/2 colocalization with TH+ neurons, and efficiency of deletion is shown in the graph (*C*) (proportion of TH+ neurons that coexpresses FOXA1/2; control VTA = 95.8% ± 2.9, control SNc = 95.8% ± 3.6; *Foxa1/2* cKO VTA = 10.4% ± 3.6*, *Foxa1/2* cKO SNc = 1.4% ± 1.6*; $n = 3$; mean ± SEM; *$P < 0.001$ vs. control, *t* test).

accompanied by an equal change in protein levels. Protein analysis by Western blotting showed that TH protein levels were indeed down-regulated in mDA neurons of adult *Foxa1/2* cKO mice (Fig. 2*B*). The activity of TH can be modulated by phosphorylation, and phospho-serine 40 TH (pSer40 TH) represents an active form of the enzyme (28). We found that, in *Foxa1/2* cKO mice, there was also a small but significant reduction in the amount of pSer40 TH, normalized to the total amount of TH

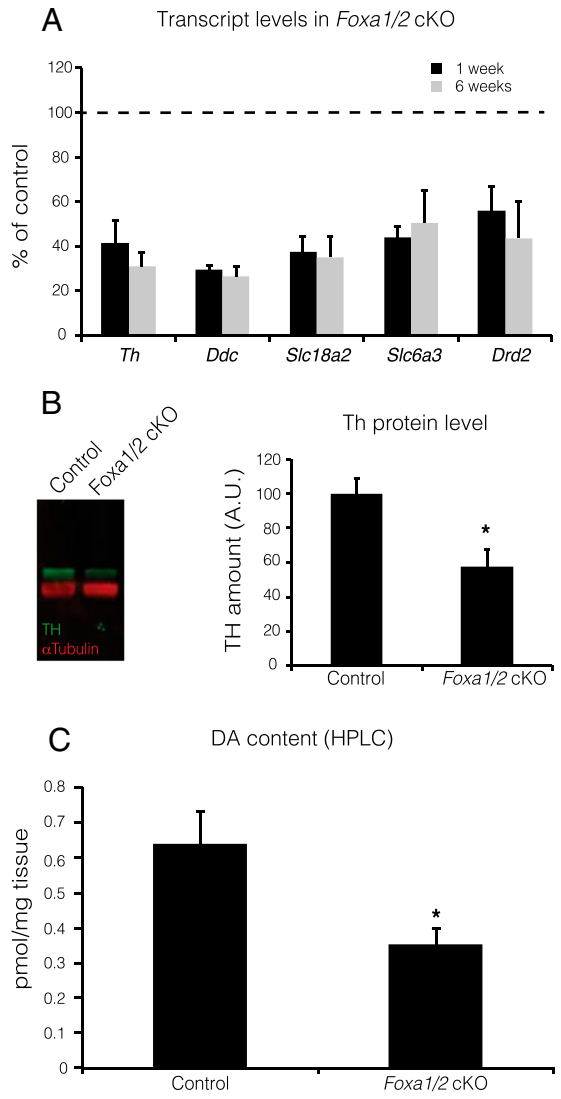

Fig. 2. Absence of FOXA1/2 leads to decreased expression of DA neuron-enriched transcripts, TH protein level, and DA content. DA neuron-enriched transcript levels in adult *Foxa1/2* cKO, at 1 and 6 weeks after tamoxifen injections, were quantified by rt-qPCR (*A*). Levels are expressed as percentage change of *Foxa1/2* cKO vs. controls (all data points P value < 0.05 vs. control; $n = 3$; t test). TH protein levels were quantified by Western blotting and a representative blot for TH and α-TUBULIN, used as loading control, is depicted in *B*. Bar graph, obtained by densitometric analysis of Western blot data, shows TH protein amount in adult *Foxa1/2* cKO compared with control mice. Data are expressed as percentage change of adult *Foxa1/2* cKO vs. controls (*B*, graphs) (TH protein amount in adult *Foxa1/2* cKO mice vs. control = 57.6 ± 10.1*; $n = 4$; *$P < 0.02$ vs. control, t test). Absolute DA content was quantified by HPLC in both control and *Foxa1/2* cKO mice (*C*) [picomoles per milligram of tissue control = 0.63 ± 0.09 ($n = 4$), *Foxa1/2* cKO = 0.35 ± 0.05* ($n = 6$); *$P < 0.02$ vs. control, t test]. All data are presented as mean ± SEM.

(Fig. S2). Down-regulation of TH and *Ddc* and a reduction of pSer40 TH converge to suggest that the ability of mDA neurons to synthesize DA might be impaired in adult *Foxa1/2* cKO mice. Accordingly, we found a statistically significant reduction in overall DA content in the forebrain of adult *Foxa1/2* cKO mice determined by HPLC (Fig. 2*C*). Together, these data demonstrate that FOXA1/2 are necessary for manifestation of some of the core molecular and neurochemical features of adult mDA neurons.

DA Transmission Shows Deficits Restricted to Dorsal Striatum of *Foxa1/2* cKO Mice. Having established cellular and functional differences in mDA neurons of adult *Foxa1/2* cKO mice compared with control animals, we investigated whether these changes resulted in changes to DA transmission in striatal target areas. We detected DA transmission using fast-scan cyclic voltammetry (FCV) at carbon fiber microelectrodes, which detects evoked DA release with subsecond resolution and in local subterritories. In the dorsal striatum, mean peak extracellular concentrations of DA ($[DA]_o$) evoked by single electrical stimulus pulses (0.2 ms) were significantly lower in adult *Foxa1/2* cKO compared with control animals (Fig. 3*A*). However, in the ventral striatum including nucleus accumbens, no differences in evoked $[DA]_o$ between *Foxa1/2* cKO and control mice were observed. The deficit in DA release in dorsal striatum was found to be restricted to dorsolateral striatum (Fig. 3*B*) and is likely the result of locally reduced DA content observed in dorsal striatum by HPLC analysis of tissue punches taken following FCV recordings (Fig. 3*C*). The deficit in DA release in dorsal striatum is unlikely to be a result of enhanced reuptake by DAT; comparison of uptake kinetics between control and *Foxa1/2* cKO DA transients revealed significantly lower decay constants in *Foxa1/2* cKO only under conditions of partial DAT blockade and not in drug-free control conditions (Fig. 3 *D* and *E*). Deficits in DA release were observed in dorsolateral striatum for a range of stimulus frequencies (five pulses at 5, 10, 25, or 100 Hz) that span the whole spectrum of DA neuron firing rates observed in vivo (Fig. 3*F*). The short-term plasticity of DA release (reflected in the relationship of stimulus frequency to $[DA]_o$) was unchanged (Fig. 3*G*) consistent with the reduction in DA content rather than to any changes to DA release probability. We hypothesized that reduced DA release in dorsal striatum would lead to reduced basal stimulation of postsynaptic neurons in this region. Previous studies have shown that *Fos* levels can be used as a marker of neuronal activity (29–33). We used *Fos* transcript levels as a mean to monitor neuronal activity of postsynaptic striatal neurons (33). rt-qPCR analysis revealed that dorsal striatal postsynaptic neurons in *Foxa1/2* cKO mice showed decreased *Fos* transcripts compared with control neurons. In comparison, ventral striatal postsynaptic neurons only showed a marginal decrease in *Fos* transcripts, which did not reach statistical significance (Fig. 3*H*).

Differential Loss of DA Neuron-Enriched Transcripts in the Midbrain of Adult *Foxa1/2* cKO Mice. Previous studies have established that SNc neurons predominantly innervate the dorsal striatum, whereas VTA neurons primarily target the ventral striatum (1, 25). Because we found a region-specific effect of reduced DA release and postsynaptic neuronal activity in the dorsal striatum, we determined whether these defects correlated with differences in the transcript levels of DA neuron-enriched genes between SNc and VTA. Using laser-assisted microdissection, we further dissected the mDA region into areas enriched in VTA or SNc neurons, and isolated RNA from these two areas, 4 weeks after tamoxifen injections. We validated our dissection protocol and ability to segregate VTA and SNc subgroups by checking whether the transcript levels of *Otx2*, a VTA-specific neuronal marker (34), was enriched in our VTA preparation. Our rt-qPCR analysis found the *Otx2* mRNA levels in the VTA to be higher than in the SNc of control mice (*Otx2* levels in SNc expressed as percentage of VTA levels = 34.8 ± 4.5; $n = 4$; $P < 0.0001$, t test). When we analyzed the expression of DA neuron-enriched genes in the VTA and SNc, we found that *Th*, *Ddc*, *Slc18a2*, and *Drd2* transcripts were down-regulated in the SNc but not in the VTA of adult *Foxa1/2* cKO mice, compared with the levels of control mice (Fig. 4*A*). The only transcript that was significantly changed in the VTA as well as in the SNc was *Slc6a3* (Fig. 4*A*). In addition, we quantified the expression levels of *Pitx3* and *Nr4a2*, two transcription factors also expressed in adult mDA neurons (22, 35). We found that neither *Pitx3* nor *Nr4a2* expression

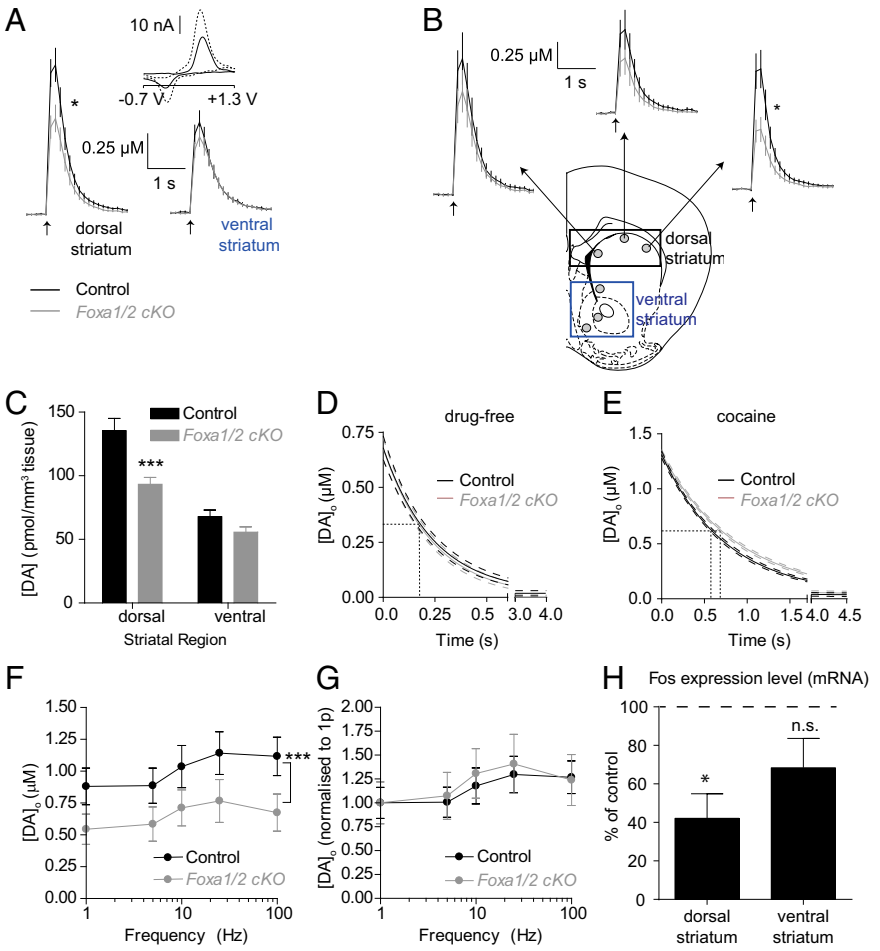

Fig. 3. Adult *Foxa1/2* cKO mice show DA transmission deficits in the dorsal striatum. (*A*) Mean extracellular DA concentration ($[DA]_o$) profiles vs. time following single-pulse stimulation (↑200 μs, 600 μA) in dorsal (*Left*) or ventral striatum (*Right*) of control (black) and *Foxa1/2* cKO (gray) mice. Mean peak evoked $[DA]_o$ was significantly lower in *Foxa1/2* cKO (0.7 ± 0.10 μM) compared with controls (1.1 ± 0.12 μM; $^*P < 0.05$; unpaired *t* test; $n = 36$; $n = 6$) in dorsal striatum but was not significantly different in ventral striatum ($P > 0.05$; unpaired *t* test; $n = 36$; $n = 6$). (*B*) FCV recording sites include three dorsal and three ventral striatum recordings. Mean $[DA]_o$ vs. time plots from individual dorsal striatum recording sites from *Foxa1/2* cKO and control mice highlights more prominent $[DA]_o$ deficit in dorsolateral striatum (dorsolateral striatum, $^*P < 0.05$; dorsomedial and dorso-mid striatum, $P > 0.05$; unpaired *t* test; $n = 12$ per region). (*C*) Mean DA content (picomoles per cubic millimeter of tissue) of *Foxa1/2* cKO mice was significantly lower than control mice in dorsal striatum ($P < 0.05$, unpaired *t* test; $n = 12$; $n = 6$) but not in ventral striatum ($P > 0.05$, unpaired *t* test; $n = 12$; $n = 6$). Exponential curve fit to the decay phases of DA transients matched for concentration, following 5p 25-Hz stimulation in dorsolateral striatum in (*D*) drug-free conditions or (*E*) partial DAT blockade (cocaine, 5 μM). In drug-free conditions, there is no detectable difference in the decay constants between control and adult *Foxa1/2* cKO conditions [*D*; *k* values: 4.1 s^{-1}, control, vs. 4.2 s^{-1}, Foxa1/2 cKO; $F_{(1,352)} = 0.02$, $P > 0.05$]. In partial DAT blockade, decay constants for *Foxa1/2* cKO transients are significantly decreased compared with control [*E*; *k* values: 1.3 s^{-1}, control, vs. 1.1 s^{-1}, *Foxa1/2* cKO; $F_{(1,422)} = 9.34$, $P < 0.01$], which corresponds to a slight increase in half-life from 0.58 to 0.69 s. Dashed lines are half-lives, and dotted lines are 95% confidence intervals. (*F*) Mean peak $[DA]_o$ ± SEM vs. frequency during five pulse trains (1–100 Hz) in dorsolateral striatum reveals overall significantly lower $[DA]_o$ in *Foxa1/2* cKO compared with control mice ($P < 0.001$; two-way ANOVA; $n = 12$ per frequency per genotype); however, relationship between stimulation frequency and mean peak $[DA]_o$ between genotypes (*G*) is not significantly different. Data are expressed as mean ± SEM, *n* represents number of observations, and *N* represents number of mice. (*H*) *Fos* was used as a marker of basal striatal neuronal activity. rt-qPCR was used to quantify *Fos* expression levels in the dorsal and ventral striatum of both control and adult *Foxa1/2* cKO mice. Data are presented as percentage change of *Foxa1/2* cKO vs. matching region in control striata (dorsal striatum = 42.1 ± 12.8*, $n = 4$; ventral striatum = 68.4 ± 15.2, $n = 5$, not significant; mean ± SEM; $^*P < 0.05$; *t* test).

was affected in the VTA and SNc of adult *Foxa1/2* cKO mice (Fig. 4*A*).

We also quantified the fluorescence intensity of TH immunoreactivity in the VTA and SNc of control and *Foxa1/2* cKO mice. Consistent with the rt-qPCR data, there was a significant reduction of intensity of TH immunoreactivity only in SNc neurons (Fig. 4*B*). These data are in agreement with the dorsoventral differences in DA release. Taken together, our data strongly suggest that a change in DA biosynthesis in the SNc leads to reduced DA content and consequently less DA released into the dorsal striatum.

We also assessed whether deletion of FOXA1/2 led to the loss of mDA neurons in our model. For this purpose, we used control and *Foxa1/2* cKO mice expressing the reporter YFP upon tamoxifen-mediated recombination. We found that both the total number of YFP-positive neurons and the percentage of YFP neurons expressing TH, were similar between control and adult *Foxa1/2* cKO animals 4 weeks after tamoxifen injections (Fig. S3 *A* and *B*). These results show that the changes in DA neuron-enriched transcript levels are not accompanied by any loss of mDA cells in adult *Foxa1/2* cKO mice.

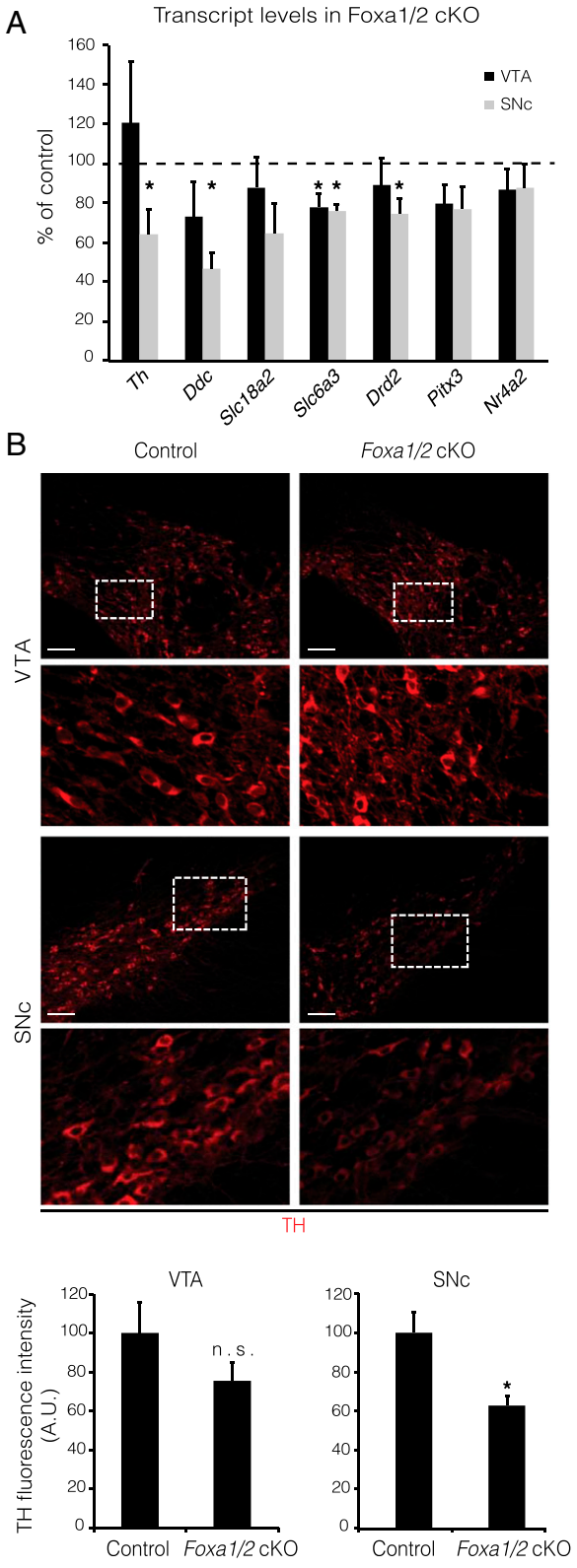

Fig. 4. Adult *Foxa1/2* cKO mice show differential reduction of DA neuron-enriched transcripts and TH levels, between the SNc and VTA. DA neuron-enriched transcript levels in VTA and SNc of control and adult *Foxa1/2* cKO mice were quantified by rt-qPCR 4 weeks after tamoxifen injections (*A*). Levels are expressed as percentage change of *Foxa1/2* cKO vs. controls ($n = 3$; mean ± SEM; $^*P < 0.05$ vs. control, *t* test). TH immunofluorescence was quantified in the VTA and SNc neurons of control and adult *Foxa1/2* cKO mice (*B*). Pictures show representative low-magnification images of TH immunoreactivity, with regions within the frames magnified. (Scale bars: 100 μm.) Bar graphs show the quantification of TH immunofluorescence levels in the VTA and SNc ($n = 3$; mean ± SEM; $^*P < 0.05$ vs. control, *t* test).

Burst Firing of mDA Neurons Is Reduced in Vivo After Deletion of FOXA1/2. Next, we investigated whether reduced DA neurotransmission in the dorsal striatum is accompanied by changes in electrophysiological properties of mDA neurons in adult *Foxa1/2* cKO mice. We made extracellular in vivo recordings of the action potentials fired by individual mDA neurons located in the SNc of anesthetized control and adult *Foxa1/2* cKO mice. Following recording, each neuron was juxtacellularly labeled to confirm its location and DAergic identity (by expression of TH; Fig. 5 *A–D*). We first examined the effects of FOXA1/2 deletion on SNc neuron firing rate and regularity. The firing rate of SNc neurons in adult *Foxa1/2* cKO mice was not significantly different from control mice (Fig. 5*H*). However, there was a significant increase in the firing regularity of SNc neurons compared with controls (assessed using CV2; Fig. 5*G*). SNc neurons can fire in different "modes," going from very regular firing (low CV2) to firing bursts of action potentials (high CV2) (36). Consequently, a decrease in firing variability could be due to a reduction in burst firing. We therefore examined the frequency of burst firing in SNc neurons; adult *Foxa1/2* cKO mice showed a significant reduction in the occurrence of bursts (Fig. 5 *E*, *F*, *K*, and *L*). The reduction of burst firing in adult *Foxa1/2* cKO mice was also reflected in the overall firing pattern as evinced by autocorrelation histograms. Firing patterns of SNc neurons in control mice could be almost evenly divided into those that were regular, irregular, or bursty (Fig. 5*I*). However, this heterogeneity in firing was heavily biased toward regular firing in adult *Foxa1/2* cKO mice, with only one neuron characterized as bursty (Fig. 5*J*). These findings suggest that the FOXA1/2 transcription factors are required for the maintenance of appropriate firing patterns of SNc neurons in vivo.

Adult *Foxa1/2* cKO Mice Display Feeding Deficits. The data presented above demonstrate that FOXA1/2 deletion results in impaired DA transmission in the dorsal striatum and reduced burst firing of SNc DAergic neurons. These changes in DAergic circuit function in the *Foxa1/2* cKO animals were accompanied by a severe weight loss that started at 3 weeks after tamoxifen treatment. Weight differences became significant 4 weeks after tamoxifen injections (Fig. 6*A*). This phenotype was irreversible and the trend continued until the mice became hunched and runted. Eventually, 93.2% of adult *Foxa1/2* cKO mice ($n = 74$) died between 6 and 7 weeks after tamoxifen injections. To further confirm that the weight loss phenotype is due to *Foxa1/2* deletion we also injected tamoxifen into double heterozygous $Foxa1^{flox/+};Foxa2^{flox/+}$ and $Slc6a3^{CreERT2/+};Foxa1^{flox/+};Foxa2^{flox/+}$ mice at 8 weeks of age and monitored body weight up to 7 weeks later. These additional control mice did not show any loss of body weight (Fig. S4). These data demonstrate that tamoxifen injections in adult mice heterozygous for FOXA1 and FOXA2 at 8 weeks of age did not lead to aphagic phenotype during the 1–7 weeks post-tamoxifen treatment.

DAergic signaling in the brain is important for the engagement of goal-directed behavior. Classically, VTA neurons projecting to the nucleus accumbens have been linked to reward/motivation mechanisms, whereas SNc neurons are more often associated with motor control. Nevertheless, this functional segregation has been challenged and it is becoming apparent that SNc neurons projecting to the dorsal striatum are also linked to the motivation to engage in goal-directed behaviors, such as feeding and drinking (37). Given the involvement of the nigrostriatal pathway in feeding behavior, and the evidence that DA signaling is specifically impaired in the dorsal striatum (i.e.,

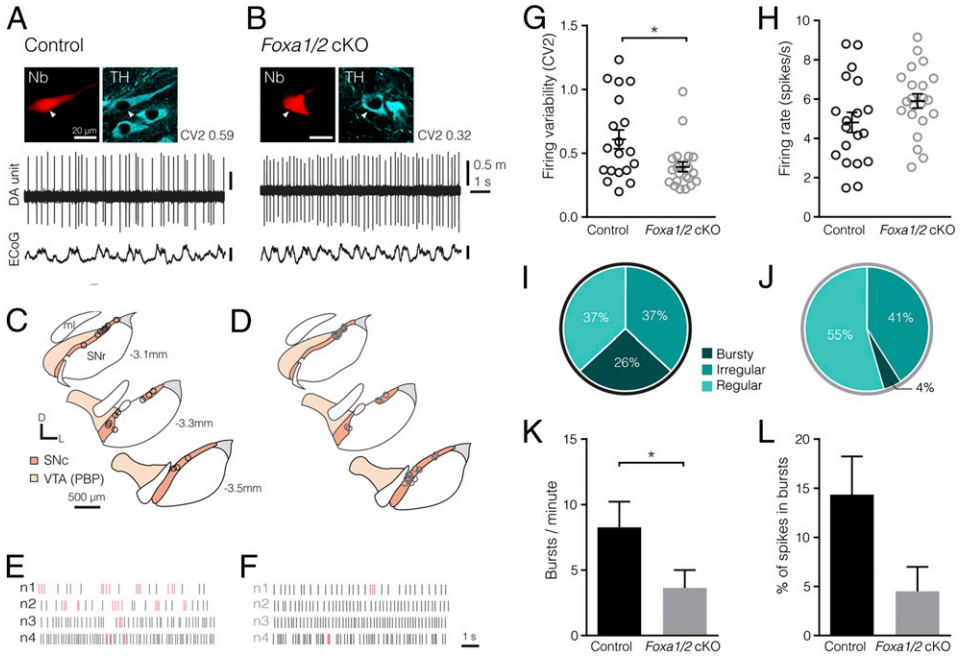

Fig. 5. SNc DAergic neurons of adult *Foxa1/2* cKO mice show a reduction in burst firing in vivo. Spontaneous activity of identified DAergic SNc neurons in control (*A*) and adult *Foxa1/2* cKO mice (*B*) is shown during robust cortical slow-wave activity [measured in the electrocorticogram (ECoG)]. Following recording, individual neurons were juxtacellularly labeled with Neurobiotin (Nb) and confirmed to be DAergic by expression of TH immunoreactivity. *C* and *D* show coronal schematics with locations of recorded and labeled DA neurons for control (*C*) and adult *Foxa1/2* cKO mice (*D*) on three rostrocaudal levels (distance caudal to bregma shown in *C*). D, dorsal; L, lateral; ml, medial lemniscus; PBP, parabrachial pigmented area of the VTA; SNc, substantia nigra pars compacta; SNr, substantia nigra pars reticulata (adapted from ref. 82). *E* and *F* are example raster plots denoting 10 s of spike firing of four example neurons from each genotype (mean CV2 of four example neurons: control = 0.65; *Foxa1/2* cKO = 0.35). Spikes detected as occurring within bursts by Gaussian Surprise are highlighted in red. Mean firing variability (*G*) and firing rate (*H*) of SNc DA neurons (control, $n = 19$; *Foxa1/2* cKO, $n = 22$; $^*P < 0.05$, Mann–Whitney rank sum test). *I* and *J* show relative distribution of autocorrelation histogram-based firing pattern classification in control (regular: 37%, $n = 7$; irregular: 37%, $n = 7$; bursty: 26%, $n = 5$) (*I*) and adult *Foxa1/2* cKO mice (regular: 55%, $n = 12$; irregular: 41%, $n = 9$; bursty: 4%, $n = 1$) (*J*). Mean number of bursts per minute as detected by Robust Gaussian Surprise (RGS) and mean percentage of spikes occurring within bursts ($^*P < 0.05$, Mann–Whitney rank sum test) are shown in *K* and *L*. Data in *G*, *H*, *K*, and *L* are displayed as mean ± SEM.

SNc target area) of adult *Foxa1/2* cKO mice, we hypothesized that the weight loss was due to feeding deficits. We therefore housed the mice individually in metabolic cages and quantified the amount of food and water consumed within 24 h. Adult *Foxa1/2* cKO mice showed a strong feeding deficit from week 3 after FOXA1/2 deletion, when the food intake, normalized to their body weight, dropped to 50% compared with control mice (Fig. 6*B*). This temporal kinetic correlates well with the weight loss described above, which also started in the third week after tamoxifen administration. Similarly, adult *Foxa1/2* cKO mice also showed decreased water intake by week 3 (Fig. 6*C*). Interestingly, adult *Foxa1/2* cKO mice also showed slightly reduced drive for rewarding stimuli. We assessed anhedonia by measuring preference to drink a sweetened solution (sucrose preference test) and *Foxa1/2* cKO displayed reduced preference for sucrose following repeated exposure (Fig. 6*D*).

Abnormal DA signaling in the striatum has been linked to feeding deficits that are accompanied by an overall hypoactivity (37–39). To distinguish between the possibility of feeding deficits per se and decreased food intake because of compromised motor functions and/or basal activity, we tested home cage activity and performed rotarod and grip strength assays. We chose home cage activity to minimize potential confounding factors due to altered anxiety levels and exploratory behavior of mice in an open-field arena (40). Home cage activity was assessed at three time points during the dark phase (1 h after lights off, 1 h in the middle of the dark phase, and 1 h before lights on, across a single 24-h time period). This behavioral task revealed no differences between adult *Foxa1/2* cKO mice and control mice, either in spontaneous locomotion, quantified as the total distance moved in the arena (Fig. 6*E*), or in the amount of entries to the feeding zone (Fig. 6*F*). We also tested motor coordination on an accelerating rotarod, and both control and adult *Foxa1/2* cKO mice were equally able to learn and perform the task (Fig. 6*G*). Finally, muscle function was quantified using the grip strength test, and no differences were detected in either the forelimb or hindlimb of adult *Foxa1/2* cKO mice compared with controls (Fig. 6*H*). These data collectively demonstrate that persistent FOXA1/2 expression in mDA neurons controls feeding behavior in adult mice. Because spontaneous locomotion, motor coordination, and muscle function are not affected in adult *Foxa1/2* cKO mice, the feeding deficit is unlikely to be due to overall hypoactivity or inability to perform the task.

L-DOPA Treatment Delays Weight Loss in Adult *Foxa1/2* cKO Mice. Having shown that FOXA1/2 positively regulate DAergic properties (Fig. 2) in adult mDA neurons and that the total DA amount is diminished in the dorsal striatum, we sought to rescue the survival of adult *Foxa1/2* cKO mice by increasing DA content with L-DOPA, thus bypassing the TH-mediated rate-limiting step in DA biosynthetic pathway. We injected 50 mg/kg L-DOPA intraperitoneally or the equivalent volume of vehicle (ascorbic acid/PBS), twice a day from the second week to the fifth week after tamoxifen administration. This dose has previously been shown to increase DA levels and lead to functional changes (38, 39, 41, 42). L-DOPA did not affect the weight of control mice, as demonstrated by the similar growth curves of control mice treated with L-DOPA or vehicle (Fig. 7), whereas vehicle-treated *Foxa1/2* cKO mice showed a pronounced weight loss. L-DOPA treatment over 3 weeks (second to fifth week after tamoxifen

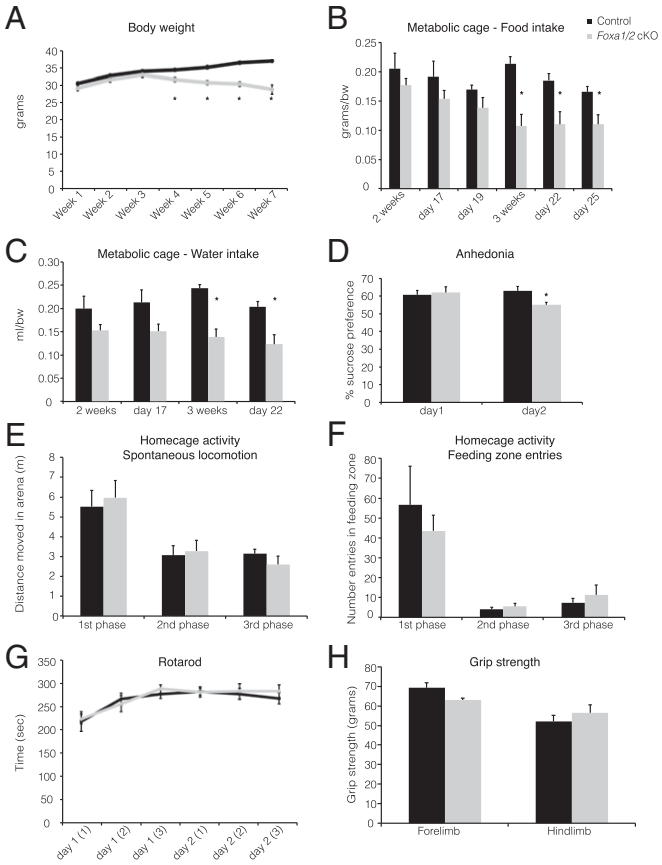

Fig. 6. Adult *Foxa1/2* cKO mice show weight loss and are characterized by reduced feeding and drinking behavior, which is accompanied neither by hypoactivity nor motor dysfunction. Data relative to control and adult *Foxa1/2* cKO mice are shown in black and gray, respectively. *A* shows body weight in grams, recorded weekly after tamoxifen injection. Each data point represents mean ± SEM ($n = 8$; $^*P < 0.05$ vs. control, two-way ANOVA followed by Sidak's multiple-comparison posttest). Feeding and drinking behavior, after tamoxifen injections, were assessed by housing the mice into metabolic cages. Food (*B*) and water (*C*) intake were quantified and are expressed as grams of food/body weight and milliliter of water/body weight, respectively (food intake: $n = 6$; $^*P < 0.001$ vs. control, two-way ANOVA followed by Sidak's multiple-comparison posttest; water intake: $n = 6$; $^*P < 0.05$ vs. control, two-way ANOVA followed by Sidak's multiple-comparison posttest). *D* shows quantification of sucrose preference test, following repeated exposure (percentage sucrose preference: control, $n = 10$; *Foxa1/2* cKO, $n = 9$; $^*P < 0.05$ vs. control, *t* test). Overall activity was assessed in home cages. Both spontaneous locomotion (total distance moved in meters) and number of entries to the feeding zone, across three time points during the dark phase, were calculated (*E* and *F*) (no statistical difference between groups, $n = 10$). Motor coordination was tested by rotarod. Latency to fall was scored in seconds (*G*) (no statistical difference between groups; control, $n = 10$; *Foxa1/2* cKO, $n = 9$). Grip strength was quantified for both forelimbs and hindlimbs of control and cKO mice (*H*). Grip strength is expressed in grams (no statistical difference between groups; control, $n = 10$; *Foxa1/2* cKO, $n = 9$). All data are presented as mean ± SEM.

injections) stabilized the body weight of adult *Foxa1/2* cKO mice over several weeks and delayed significant weight loss for up to 9 weeks after tamoxifen administration. Altogether, these data demonstrate that L-DOPA treatment delays the onset of weight loss and rescues the lethality observed in adult *Foxa1/2* cKO mice.

Discussion

In this study, we discovered a novel role for FOXA1/2 in maintaining DA biosynthesis in mDA neurons and DA transmission in the striatum. The reduction in DA content and transmission seen after conditional knockout of *Foxa1/2* during adulthood is accompanied by loss of burst-firing activity in mDA neurons. These defects result in changes in feeding behavior that is incompatible with life in adult mice.

Our study shows that FOXA1/2 are required to maintain correct levels of *Th*, *Ddc*, *Slc18a2*, *Slc6a3*, and *Drd2* transcripts in adult mDA neurons. During prenatal development, FOXA2 has previously been shown to cooperate with NURR1 to regulate the expression of *Th*, *Ddc*, and *Slc18a2* through direct binding of transcriptional regulatory sequences of these three genes (23, 43). It is therefore possible that FOXA1/2 are still required to cooperate with NURR1 to regulate gene expression in adult mDA neurons. Loss of FOXA1/2 in mDA neurons during adulthood leads to only partial reduction of DA-enriched transcripts, in contrast to the complete loss of these transcripts when FOXA1/2 are inactivated in the same neurons from embryonic day 13.5 onward (23). This difference may be due to the maintenance of PITX3 expression in adult *Foxa1/2* cKO mice (Fig. 4*A*), whereas PITX3 expression is lost in *Slc6a3Cre;Foxa1*$^{flox/flox}$*;Foxa2*$^{flox/flox}$ mice (23). As PITX3 also synergizes with NURR1 to regulate many genes that have enriched expression in mDA neurons (44, 45), it may be able to compensate partially for the loss of FOXA1/2 in adult mDA neurons. Regardless of the exact molecular mechanism of regulation, our study clearly demonstrates that FOXA1/2 are needed to maintain correct levels of DA neuron-enriched transcripts. Most importantly, absence of FOXA1/2 and the concomitant dysregulation of gene expression results in reduced DA content in the striatum.

In our adult *Foxa1/2* cKO mice, reduction in DA content likely resulted in decreased DA transmission and postsynaptic neuronal activity (reduction in *Fos* mRNA levels) in the dorsal but not the ventral striatum. Notably, this dorsoventral difference in DA transmission in the striatum was paralleled by SNc-specific differences in gene expression in the midbrain. Surprisingly, ablation of FOXA1/2 in the midbrain specifically affected *Th* transcripts in the SNc only, whereas our earlier work showed that loss of FOXA1/2 during late development affected the expression of DA neuron-enriched genes in the majority of mDA neurons (23). Our finding is consistent with the observation of normal DA transmission in the ventral striatum, which receives projection from the VTA, where *Th* expression is maintained. These results suggest that FOXA1/2 are not required for regulating DA-specific properties in VTA neurons, perhaps due to a VTA-specific mechanism that is able to compensate for the function of FOXA1/2 deletion in these neurons. It is noteworthy that mutations in other uniformly expressed transcription factors in SNc and VTA neurons have also resulted in defects specific to SNc neurons, suggesting that these neurons are more vulnerable to changes from normal homeostasis (46–49).

Our adult *Foxa1/2* cKO mice also show deficits in firing pattern of SNc neurons, which may also contribute to dysregulated DA signaling in the striatum. Presently, we cannot distinguish between a cell-autonomous role of FOXA1/2 in mediating burst firing and/or an indirect role through maintenance of DA tone. One possibility is that absence of FOXA1/2 in adult mice may alter the expression of proteins determining intrinsic cellular excitability (e.g., ion channels, scaffolding protein, signaling protein), and therefore affects both the ability of these neurons to generate physiological firing patterns and to respond to endogenous afferent inputs. Burst firing in mDA neurons is dependent on afferent inputs (50), as demonstrated by ex vivo midbrain preparations, which lack the burst-firing component (51). One major contributor to the burst firing displayed by mDA neurons is the glutamatergic input (52, 53), although GABAergic innervation can also modulate burst firing (54). It is tempting to hypothesize that the absence of burst firing is due to altered control of inputs to mDA neurons. mDA neurons project and receive, among others, innervation from the striatum (25, 55),

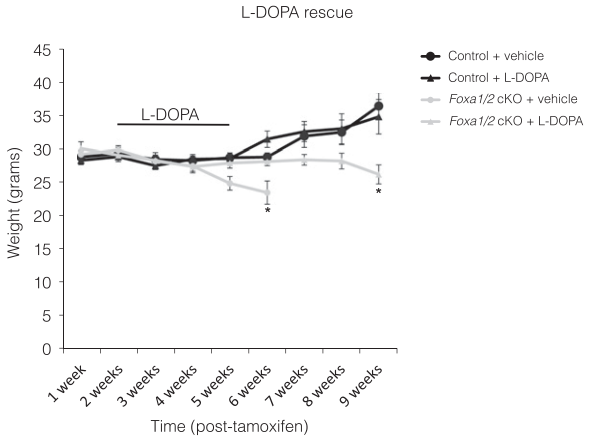

Fig. 7. Weight loss can be rescued by L-DOPA treatments. Graph shows body weight in grams, recorded weekly after tamoxifen injection. L-DOPA (or vehicle) was delivered intraperitoneally, twice a day between the second and fifth week after tamoxifen injections. Each data point represents mean ± SEM (*$P < 0.05$ vs. control, two-way ANOVA followed by Tukey's multiple-comparison posttest; $n = 5$).

prefrontal cortex (56, 57), and peduncolopontine tegmental nucleus (58). In turn, endogenous DA can directly influence mDA neurons and their firing via a network feedback mechanism (51, 59). These evidence raise the possibility that reduced DA tone and transmission may influence mDA firing properties in our mutant mice by dysregulating glutamatergic/GABAergic afferent input. Another interesting possibility is that FOXA1/2 mutant mice fail to appropriately integrate signaling arising from the action of orexigenic peptides (60) and/or inputs from brain centers regulating feeding (61, 62), thus failing to sense the physiological energetic state.

Our mouse model showed a striking aphagic phenotype after FOXA1/2 deletion and, ultimately, death 6–7 weeks after tamoxifen administration in the majority of adult mice [a small proportion of mice (6.8%, $n = 74$) are able to bypass this lethality]. Adult *Foxa1/2* cKO mice also show reduced preference for a sweetened solution, which may be indicative of a reduced drive for rewarding stimuli. DA role in feeding is well documented as DA-deficient mice are hypoactive and hypophagic (38, 39), pharmacological blockade of DA signaling in the striatum correlates with impaired feeding (63), and restoration of DA signaling in DA-deficient mice promotes feeding behavior (64). To distinguish direct roles of FOXA1/2 in regulating feeding behavior from motor activity, we have conducted motor function and activity assays. Our behavioral analyses rule out both hypoactivity (home cage) and gross motor function deficit (rotarod, grip strength). Because adult *Foxa1/2* cKO mice do not show motor impairment, our model, featuring feeding deficit and anhedonia, suggests that FOXA1/2 control feeding behavior by impairing motivation and goal-directed behaviors.

Classically, the mesocorticolimbic pathways have been associated with cognitive functions including motivation and goal-directed behaviors, whereas the nigrostriatal pathway regulates motor functions. However, this clear dichotomy has been challenged by studies showing that SNc neurons are also linked to reward and aversion mechanisms (65), addiction (66), learning (67), and motivation to feed (37). DA also contributes to maintain the value of rewarding stimuli, leading to reward-seeking behavior (68, 69), and serves as a modulator of food seeking (70). The different modalities of DA release (tonic vs. phasic) are believed to lead to differential DA receptor occupancy in the target areas, with phasic release thought to increase D1 receptor occupancy (71) and to subserve neuronal coding for different behaviors (72). For example, a burst-firing mode has been shown to be sufficient for behavioral conditioning (conditioned place preference) (73) and to be necessary for learning of cue-dependent learning tasks (53). Furthermore, reward-related stimuli presentation (74) and food restriction (75) correlate with burst-firing increase, and burst firing in a subset of SNc neurons mediates novelty-induced exploration (76).

Because other genetic mouse models with a moderate reduction in DA content similar to that of adult *Foxa1/2* cKO mice do not lead to an aphagic phenotype (22, 77), we therefore speculate that our model represents a scenario whereby a 50% reduction in DA content in combination with a reduction of burst firing together impair both the quantity and the temporal control of DA release in the striatum. This dysregulation primarily contributes to aphagia due to lack of motivation to feed/drink (37), whereas overall activity/motor function remains unaffected. L-DOPA rescue of aphagia demonstrates that this phenotype is DA dependent in adult *Foxa1/2* cKO mice. In addition, L-DOPA treatment has been shown to inhibit or excite mDA neurons, depending on the experimental conditions (59, 78, 79). Interestingly, in the presence of DRD2 blocker, L-DOPA has an excitatory effect on SNc neurons (78). In our mouse model, characterized by reduced *Drd2* transcripts, L-DOPA may exert an excitatory effect. Given the dual role of L-DOPA on mDA neuron properties, we hypothesize that L-DOPA treatments may rescue aphagia by increasing both DA production and firing rates of mDA neurons in adult *Foxa1/2* cKO mice.

Understanding how DAergic features are maintained during adulthood is important in light of the role of mDA neurons in diverse cognitive functions and in Parkinson's disease. Our study proves that FOXA1/2 are not only required to determine DAergic features during development but are also crucial to maintain these properties and DA transmission in adult mDA neurons. It is noteworthy that a recent study using the same mouse model maintained in a different genetic background (C57Bl6N vs. our outbred background) showed that absence of FOXA1/2 in adult mDA neurons results in late (78 weeks after *Foxa1/2* deletion) degeneration of mDA neurons (80), but this paper did not describe the analysis of mutant phenotypes at earlier time points, as described in our study. As 93.2% ($n = 74$) of our *Foxa1/2* cKO mutant animals died by 6–7 weeks after tamoxifen treatment, we have examined a possible degeneration of mDA neurons by determining their total number only at 4 weeks after tamoxifen treatment. We found no significant difference in cell numbers in *Foxa1/2* cKO compared with control mice at this stage (Fig. S3). This result agrees with the data reported by Domanskyi et al. (80), which showed that total mDA neuronal number in adult *Foxa1/2* cKO mice (in a C57Bl6N background) was still normal at 24 weeks after tamoxifen treatment. It will be interesting to determine whether neurodegeneration of mDA neurons is also observed in *Foxa1/2* cKO animals in an outbred background at later stages. However, this experiment is still pending given that the majority of these mice die by 4 months of age.

In conclusion, our study identifies FOXA1/2 as novel transcription factors in mDA neurons with a role in stimulating feeding behavior, by involving the nigrostriatal pathway in the midbrain. Future studies will focus on determining how FOXA1/2 contribute to the regulation of burst-firing activity in mDA neurons and whether they are required for the response of mDA neurons to orexigenic peptides.

Materials and Methods

Mice. Research involving animals has been approved by the Home Office–Secretary of State (ref. no. 80/2550) and Institutional Animals Welfare and Ethical Review Body of The Francis Crick Institute, which has been approved by the Home Office as a breeding, supplying, and research establishment (ref. no. 70/9092). All procedures were carried out in accordance with the Animals

(Scientific Procedure) Act of 1986. Mice were maintained on a 12-h light/dark cycle with water and food ad libitum. *Foxa1/2*$^{flox/flox}$ mice were generated as previously described (19). *Foxa1/2*$^{flox/flox}$ mice were crossed with *Slc6a3*$^{CreERT2/+}$ male mice (81) to generate *Slc6a3*$^{CreERT2/+}$;*Foxa1/2*$^{flox/flox}$ mice and were maintained in an outbred MF1 background. As control, we used littermates harboring only the floxed alleles. We confirmed by Western blotting that FOXA1/2 protein levels are similar in wild-type mice and mice harboring *Foxa1/2* floxed alleles (Fig. S5). Pharmacological treatments are described in *SI Materials and Methods*.

Immunohistochemistry of Brain Sections. Mice were transcardially perfused with ice-cold heparin followed by 4% (wt/vol) paraformaldehyde (PFA) in PBS, pH 7.4. Brains were dissected, postfixed at 4 °C overnight in 4% PFA in PBS, and cryoprotected with 30% (wt/vol) sucrose in PBS for 24 h. Brains were embedded in optimal cutting temperature compound (VWR International), frozen, and sectioned in a cryostat (Leica). The 35-μm sections were collected with the aid of a fine brush in PBS as floating sections, washed three times, and blocked in 1% BSA, 0.2% Triton X-100 (TX100) in PBS. Primary antibody incubation was performed overnight at 4 °C with rabbit anti-TH (1:1,000; Pel-Freez), rat anti-DAT (1:100; Millipore), sheep anti-YFP (1:1,000; AbD Serotec), goat anti-FOXA1/2 (1:1,000; Santa Cruz), and rabbit anti-FOXA2 (1:1,000; Seven Hills). After extensive washes, sections were incubated with the appropriate secondary antibodies (1:250; Life Technologies), conjugated to fluorochromes (Alexa 488 and Alexa 594), for 1 h at room temperature. All antibodies were diluted in 1% BSA, 0.2% TX100 in PBS. Sections were washed and mounted on glass slides with mounting media containing DAPI (Vectashield). Pictures were acquired on an Axio Imager.Z2 ApoTome.2 microscope (Zeiss) equipped with an AxioCam MRm camera. Image analysis is described in *SI Materials and Methods*.

Laser-Assisted Microdissection and rt-qPCR. Mice were culled and brains were rapidly removed and snap frozen in optimal cutting temperature compound. The 14-μm sections were collected onto PEN-membrane covered glass slides (Zeiss) and stored at −80 °C until use. Sections processed for TH staining were washed and fixed in 4% PFA in PBS for 10 min at room temperature. After washes, sections were blocked with 1% BSA, 0.02% TX100 in PBS for 1 h at room temperature and incubated overnight at 4 °C with rabbit anti-TH (1:1,000; Pel-Freez). Following several washes, sections were incubated with biotinylated secondary anti-rabbit antibody (1:250; Vector Laboratories). All antibodies were diluted in 1% BSA, 0.02% TX100 in PBS. TH was immunolocalized with 3,3′-diaminobenzidine, developed by using the ABC staining kit (Vector Laboratories) following manufacturer's instruction. Unstained sections were dehydrated by incubation in ascending ethanol series prepared in diethylpyrocarbonate-treated water [50%, 75%, 90%, 100% (vol/vol)]. VTA and SNc nuclei were rapidly collected from the unstained sections by using laser-assisted microscopy (PALM MicroBeam; Zeiss). Adjacent TH-stained sections were used as a mask to identify the VTA and SNc nuclei.

Total RNA was extracted from the microdissected VTA and SNc by using the Arcturus PicoPure RNA Isolation kit (Applied Biosystems). cDNA synthesis was performed with SuperScript III First-Strand Synthesis kit, by using oligo-d(T) primers, following manufacturer's instruction (Invitrogen). Transcript levels were quantified by rt-qPCR performed with KAPA Sybr Fast rt-qPCR (Kapa Biosystems) mix in a total volume of 20 μL on a 7900HT fast real-time machine (Applied Biosystems). The threshold amplification cycles (Ct) were determined by using SDS2.3 software, and transcript levels, normalized to endogenous *Gapdh* levels, were quantified by the $2^{-\Delta\Delta Ct}$ method. Primer sequences are provided in *SI Materials and Methods*.

Western blotting, in vivo electrophysiology, FCV, and HPLC are described in detail in *SI Materials and Methods*.

Behavior. For the feeding behavior study, mice were individually housed in metabolic cages and maintained on a 12-h light/dark cycle with water and food available ad libitum. Food and water consumption was monitored regularly for the duration of the experiment. The food crumbs and water spillage that the mice produced were collected in appropriate holders to accurately measure food and water consumption across 24 h. Details of mice housing and other behavioral tests are in *SI Materials and Methods*.

ACKNOWLEDGMENTS. We thank Profs. J. Paul Bolam and Jochen Roeper for stimulating and helpful discussions. This work was supported by the Francis Crick Institute, which receives its core funding from the UK Medical Research Council (MRC), and the Wellcome Trust. In addition, this research was supported by MRC Award MC_UU_12020/5 (to P.J.M.) and the Monument Trust Discovery Award from Parkinson's UK (Grant J-0901) (to P.J.M., S.T., and S.J.C.). A.-K.K. holds an MRC studentship, and K.R.B. was awarded Parkinson's Disease UK Studentship H-1003.

1. Roeper J (2013) Dissecting the diversity of midbrain dopamine neurons. *Trends Neurosci* 36(6):336–342.
2. Wise RA (2006) Role of brain dopamine in food reward and reinforcement. *Philos Trans R Soc Lond B Biol Sci* 361(1471):1149–1158.
3. Wise RA (2004) Dopamine, learning and motivation. *Nat Rev Neurosci* 5(6):483–494.
4. Ikemoto S (2007) Dopamine reward circuitry: Two projection systems from the ventral midbrain to the nucleus accumbens-olfactory tubercle complex. *Brain Res Brain Res Rev* 56(1):27–78.
5. Iversen L, Iversen S, Dunnett S, Bjorklund A (2009) *Dopamine Handbook* (Oxford Univ Press, New York), 1st Ed.
6. Obeso JA, et al. (2010) Missing pieces in the Parkinson's disease puzzle. *Nat Med* 16(6): 653–661.
7. Milton AL, Everitt BJ (2012) The persistence of maladaptive memory: Addiction, drug memories and anti-relapse treatments. *Neurosci Biobehav Rev* 36(4):1119–1139.
8. Tye KM, et al. (2013) Dopamine neurons modulate neural encoding and expression of depression-related behaviour. *Nature* 493(7433):537–541.
9. Volkow ND, Fowler JS, Wang GJ, Swanson JM, Telang F (2007) Dopamine in drug abuse and addiction: Results of imaging studies and treatment implications. *Arch Neurol* 64(11):1575–1579.
10. Winterer G, Weinberger DR (2004) Genes, dopamine and cortical signal-to-noise ratio in schizophrenia. *Trends Neurosci* 27(11):683–690.
11. Jackson BC, Carpenter C, Nebert DW, Vasiliou V (2010) Update of human and mouse forkhead box (FOX) gene families. *Hum Genomics* 4(5):345–352.
12. Cirillo LA, et al. (2002) Opening of compacted chromatin by early developmental transcription factors HNF3 (FoxA) and GATA-4. *Mol Cell* 9(2):279–289.
13. Hannenhalli S, Kaestner KH (2009) The evolution of Fox genes and their role in development and disease. *Nat Rev Genet* 10(4):233–240.
14. Friedman JR, Kaestner KH (2006) The Foxa family of transcription factors in development and metabolism. *Cell Mol Life Sci* 63(19-20):2317–2328.
15. Ang SL (2009) Foxa1 and Foxa2 transcription factors regulate differentiation of midbrain dopaminergic neurons. *Adv Exp Med Biol* 651:58–65.
16. Lin W, et al. (2009) Foxa1 and Foxa2 function both upstream of and cooperatively with Lmx1a and Lmx1b in a feedforward loop promoting mesodiencephalic dopaminergic neuron development. *Dev Biol* 333(2):386–396.
17. Mavromatakis YE, et al. (2011) Foxa1 and Foxa2 positively and negatively regulate Shh signalling to specify ventral midbrain progenitor identity. *Mech Dev* 128(1-2): 90–103.
18. Metzakopian E, et al. (2012) Genome-wide characterization of Foxa2 targets reveals upregulation of floor plate genes and repression of ventrolateral genes in midbrain dopaminergic progenitors. *Development* 139(14):2625–2634.
19. Ferri AL, et al. (2007) Foxa1 and Foxa2 regulate multiple phases of midbrain dopaminergic neuron development in a dosage-dependent manner. *Development* 134(15): 2761–2769.
20. Doucet-Beaupré H, Lévesque M (2013) The role of developmental transcription factors in adult midbrain dopaminergic neurons. *OA Neurosci* 1(1):3.
21. Di Salvio M, et al. (2010) Otx2 controls neuron subtype identity in ventral tegmental area and antagonizes vulnerability to MPTP. *Nat Neurosci* 13(12):1481–1488.
22. Kadkhodaei B, et al. (2013) Transcription factor Nurr1 maintains fiber integrity and nuclear-encoded mitochondrial gene expression in dopamine neurons. *Proc Natl Acad Sci USA* 110(6):2360–2365.
23. Stott SR, et al. (2013) Foxa1 and foxa2 are required for the maintenance of dopaminergic properties in ventral midbrain neurons at late embryonic stages. *J Neurosci* 33(18):8022–8034.
24. Kittappa R, Chang WW, Awatramani RB, McKay RD (2007) The foxa2 gene controls the birth and spontaneous degeneration of dopamine neurons in old age. *PLoS Biol* 5(12):e325.
25. Björklund A, Dunnett SB (2007) Dopamine neuron systems in the brain: An update. *Trends Neurosci* 30(5):194–202.
26. Li ZS, Pham TD, Tamir H, Chen JJ, Gershon MD (2004) Enteric dopaminergic neurons: Definition, developmental lineage, and effects of extrinsic denervation. *J Neurosci* 24(6):1330–1339.
27. Sasselli V, Pachnis V, Burns AJ (2012) The enteric nervous system. *Dev Biol* 366(1): 64–73.
28. Dunkley PR, Bobrovskaya L, Graham ME, von Nagy-Felsobuki EI, Dickson PW (2004) Tyrosine hydroxylase phosphorylation: Regulation and consequences. *J Neurochem* 91(5):1025–1043.
29. Cohen S, Greenberg ME (2008) Communication between the synapse and the nucleus in neuronal development, plasticity, and disease. *Annu Rev Cell Dev Biol* 24:183–209.
30. Herdegen T, Leah JD (1998) Inducible and constitutive transcription factors in the mammalian nervous system: Control of gene expression by Jun, Fos and Krox, and CREB/ATF proteins. *Brain Res Brain Res Rev* 28(3):370–490.
31. Robertson GS, Vincent SR, Fibiger HC (1992) D1 and D2 dopamine receptors differentially regulate c-fos expression in striatonigral and striatopallidal neurons. *Neuroscience* 49(2):285–296.
32. Sheng M, McFadden G, Greenberg ME (1990) Membrane depolarization and calcium induce c-fos transcription via phosphorylation of transcription factor CREB. *Neuron* 4(4):571–582.
33. Yang L, Gilbert ML, Zheng R, McKnight GS (2014) Selective expression of a dominant-negative type Iα PKA regulatory subunit in striatal medium spiny neurons impairs

gene expression and leads to reduced feeding and locomotor activity. *J Neurosci* 34(14):4896–4904.
34. Di Salvio M, Di Giovannantonio LG, Omodei D, Acampora D, Simeone A (2010) Otx2 expression is restricted to dopaminergic neurons of the ventral tegmental area in the adult brain. *Int J Dev Biol* 54(5):939–945.
35. Luk KC, et al. (2013) The transcription factor Pitx3 is expressed selectively in midbrain dopaminergic neurons susceptible to neurodegenerative stress. *J Neurochem* 125(6): 932–943.
36. Grace AA, Bunney BS (1983) Intracellular and extracellular electrophysiology of nigral dopaminergic neurons—1. Identification and characterization. *Neuroscience* 10(2): 301–315.
37. Palmiter RD (2008) Dopamine signaling in the dorsal striatum is essential for motivated behaviors: Lessons from dopamine-deficient mice. *Ann N Y Acad Sci* 1129: 35–46.
38. Zhou QY, Palmiter RD (1995) Dopamine-deficient mice are severely hypoactive, adipsic, and aphagic. *Cell* 83(7):1197–1209.
39. Szczypka MS, et al. (1999) Feeding behavior in dopamine-deficient mice. *Proc Natl Acad Sci USA* 96(21):12138–12143.
40. Lad HV, et al. (2010) Behavioural battery testing: Evaluation and behavioural outcomes in 8 inbred mouse strains. *Physiol Behav* 99(3):301–316.
41. Chartoff EH, Marck BT, Matsumoto AM, Dorsa DM, Palmiter RD (2001) Induction of stereotypy in dopamine-deficient mice requires striatal D1 receptor activation. *Proc Natl Acad Sci USA* 98(18):10451–10456.
42. Kim DS, Szczypka MS, Palmiter RD (2000) Dopamine-deficient mice are hypersensitive to dopamine receptor agonists. *J Neurosci* 20(12):4405–4413.
43. Yi SH, et al. (2014) Foxa2 acts as a co-activator potentiating expression of the Nurr1-induced DA phenotype via epigenetic regulation. *Development* 141(4):761–772.
44. Jacobs FM, et al. (2009) Pitx3 potentiates Nurr1 in dopamine neuron terminal differentiation through release of SMRT-mediated repression. *Development* 136(4): 531–540.
45. Martinat C, et al. (2006) Cooperative transcription activation by Nurr1 and Pitx3 induces embryonic stem cell maturation to the midbrain dopamine neuron phenotype. *Proc Natl Acad Sci USA* 103(8):2874–2879.
46. Hegarty SV, Sullivan AM, O'Keeffe GW (2013) Midbrain dopaminergic neurons: A review of the molecular circuitry that regulates their development. *Dev Biol* 379(2): 123–138.
47. Kramer ER, et al. (2007) Absence of Ret signaling in mice causes progressive and late degeneration of the nigrostriatal system. *PLoS Biol* 5(3):e39.
48. Maxwell SL, Ho HY, Kuehner E, Zhao S, Li M (2005) Pitx3 regulates tyrosine hydroxylase expression in the substantia nigra and identifies a subgroup of mesencephalic dopaminergic progenitor neurons during mouse development. *Dev Biol* 282(2): 467–479.
49. van den Munckhof P, et al. (2003) Pitx3 is required for motor activity and for survival of a subset of midbrain dopaminergic neurons. *Development* 130(11):2535–2542.
50. Floresco SB, West AR, Ash B, Moore H, Grace AA (2003) Afferent modulation of dopamine neuron firing differentially regulates tonic and phasic dopamine transmission. *Nat Neurosci* 6(9):968–973.
51. Paladini CA, Robinson S, Morikawa H, Williams JT, Palmiter RD (2003) Dopamine controls the firing pattern of dopamine neurons via a network feedback mechanism. *Proc Natl Acad Sci USA* 100(5):2866–2871.
52. Overton PG, Clark D (1997) Burst firing in midbrain dopaminergic neurons. *Brain Res Brain Res Rev* 25(3):312–334.
53. Zweifel LS, et al. (2009) Disruption of NMDAR-dependent burst firing by dopamine neurons provides selective assessment of phasic dopamine-dependent behavior. *Proc Natl Acad Sci USA* 106(18):7281–7288.
54. Tepper JM, Lee CR (2007) GABAergic control of substantia nigra dopaminergic neurons. *Prog Brain Res* 160:189–208.
55. Watabe-Uchida M, Zhu L, Ogawa SK, Vamanrao A, Uchida N (2012) Whole-brain mapping of direct inputs to midbrain dopamine neurons. *Neuron* 74(5):858–873.
56. Land BB, et al. (2014) Medial prefrontal D1 dopamine neurons control food intake. *Nat Neurosci* 17(2):248–253.
57. Naito A, Kita H (1994) The cortico-nigral projection in the rat: An anterograde tracing study with biotinylated dextran amine. *Brain Res* 637(1-2):317–322.
58. Charara A, Smith Y, Parent A (1996) Glutamatergic inputs from the pedunculopontine nucleus to midbrain dopaminergic neurons in primates: *Phaseolus vulgaris*-leucoagglutinin anterograde labeling combined with postembedding glutamate and GABA immunohistochemistry. *J Comp Neurol* 364(2):254–266.
59. Robinson S, Smith DM, Mizumori SJ, Palmiter RD (2004) Firing properties of dopamine neurons in freely moving dopamine-deficient mice: Effects of dopamine receptor activation and anesthesia. *Proc Natl Acad Sci USA* 101(36):13329–13334.
60. Abizaid A, et al. (2006) Ghrelin modulates the activity and synaptic input organization of midbrain dopamine neurons while promoting appetite. *J Clin Invest* 116(12): 3229–3239.
61. Cone JJ, McCutcheon JE, Roitman MF (2014) Ghrelin acts as an interface between physiological state and phasic dopamine signaling. *J Neurosci* 34(14):4905–4913.
62. Egecioglu E, et al. (2011) Hedonic and incentive signals for body weight control. *Rev Endocr Metab Disord* 12(3):141–151.
63. Terry P, Gilbert DB, Cooper SJ (1995) Dopamine receptor subtype agonists and feeding behavior. *Obes Res* 3(Suppl 4):515S–523S.
64. Hnasko TS, et al. (2006) Cre recombinase-mediated restoration of nigrostriatal dopamine in dopamine-deficient mice reverses hypophagia and bradykinesia. *Proc Natl Acad Sci USA* 103(23):8858–8863.
65. Ilango A, et al. (2014) Similar roles of substantia nigra and ventral tegmental dopamine neurons in reward and aversion. *J Neurosci* 34(3):817–822.
66. Wise RA (2009) Roles for nigrostriatal—not just mesocorticolimbic—dopamine in reward and addiction. *Trends Neurosci* 32(10):517–524.
67. Robinson S, Rainwater AJ, Hnasko TS, Palmiter RD (2007) Viral restoration of dopamine signaling to the dorsal striatum restores instrumental conditioning to dopamine-deficient mice. *Psychopharmacology (Berl)* 191(3):567–578.
68. Bromberg-Martin ES, Matsumoto M, Hikosaka O (2010) Dopamine in motivational control: Rewarding, aversive, and alerting. *Neuron* 68(5):815–834.
69. Wanat MJ, Willuhn I, Clark JJ, Phillips PE (2009) Phasic dopamine release in appetitive behaviors and drug addiction. *Curr Drug Abuse Rev* 2(2):195–213.
70. Roitman MF, Stuber GD, Phillips PE, Wightman RM, Carelli RM (2004) Dopamine operates as a subsecond modulator of food seeking. *J Neurosci* 24(6):1265–1271.
71. Dreyer JK, Herrik KF, Berg RW, Hounsgaard JD (2010) Influence of phasic and tonic dopamine release on receptor activation. *J Neurosci* 30(42):14273–14283.
72. Grace AA, Floresco SB, Goto Y, Lodge DJ (2007) Regulation of firing of dopaminergic neurons and control of goal-directed behaviors. *Trends Neurosci* 30(5):220–227.
73. Tsai HC, et al. (2009) Phasic firing in dopaminergic neurons is sufficient for behavioral conditioning. *Science* 324(5930):1080–1084.
74. Hyland BI, Reynolds JN, Hay J, Perk CG, Miller R (2002) Firing modes of midbrain dopamine cells in the freely moving rat. *Neuroscience* 114(2):475–492.
75. Branch SY, et al. (2013) Food restriction increases glutamate receptor-mediated burst firing of dopamine neurons. *J Neurosci* 33(34):13861–13872.
76. Schiemann J, et al. (2012) K-ATP channels in dopamine substantia nigra neurons control bursting and novelty-induced exploration. *Nat Neurosci* 15(9):1272–1280.
77. Darvas M, Henschen CW, Palmiter RD (2014) Contributions of signaling by dopamine neurons in dorsal striatum to cognitive behaviors corresponding to those observed in Parkinson's disease. *Neurobiol Dis* 65:112–123.
78. Guatteo E, et al. (2013) Dual effects of L-DOPA on nigral dopaminergic neurons. *Exp Neurol* 247:582–594.
79. Harden DG, Grace AA (1995) Activation of dopamine cell firing by repeated L-DOPA administration to dopamine-depleted rats: Its potential role in mediating the therapeutic response to L-DOPA treatment. *J Neurosci* 15(9):6157–6166.
80. Domanskyi A, Alter H, Vogt MA, Gass P, Vinnikov IA (2014) Transcription factors Foxa1 and Foxa2 are required for adult dopamine neurons maintenance. *Front Cell Neurosci* 8:275.
81. Rieker C, et al. (2011) Nucleolar disruption in dopaminergic neurons leads to oxidative damage and parkinsonism through repression of mammalian target of rapamycin signaling. *J Neurosci* 31(2):453–460.
82. Franklin KBJ, Paxinos G (2012) *Paxinos and Franklin's the Mouse Brain in Stereotaxic Coordinates* (Academic, San Diego), 4th Ed.
83. Janezic S, et al. (2013) Deficits in dopaminergic transmission precede neuron loss and dysfunction in a new Parkinson model. *Proc Natl Acad Sci USA* 110(42):E4016–E4025.
84. Brown MT, Henny P, Bolam JP, Magill PJ (2009) Activity of neurochemically heterogeneous dopaminergic neurons in the substantia nigra during spontaneous and driven changes in brain state. *J Neurosci* 29(9):2915–2925.
85. Holt GR, Softky WR, Koch C, Douglas RJ (1996) Comparison of discharge variability in vitro and in vivo in cat visual cortex neurons. *J Neurophysiol* 75(5):1806–1814.
86. Ko D, Wilson CJ, Lobb CJ, Paladini CA (2012) Detection of bursts and pauses in spike trains. *J Neurosci Methods* 211(1):145–158.
87. Wilson CJ, Young SJ, Groves PM (1977) Statistical properties of neuronal spike trains in the substantia nigra: Cell types and their interactions. *Brain Res* 136(2):243–260.
88. Grayton HM, Missler M, Collier DA, Fernandes C (2013) Altered social behaviours in neurexin 1α knockout mice resemble core symptoms in neurodevelopmental disorders. *PLoS One* 8(6):e67114.
89. Monleon S, et al. (1995) Attenuation of sucrose consumption in mice by chronic mild stress and its restoration by imipramine. *Psychopharmacology (Berl)* 117(4):453–457.
90. Holmes A, et al. (2001) Behavioral characterization of dopamine D5 receptor null mutant mice. *Behav Neurosci* 115(5):1129–1144.
91. Whittemore LA, et al. (2003) Inhibition of myostatin in adult mice increases skeletal muscle mass and strength. *Biochem Biophys Res Commun* 300(4):965–971.

Supporting Information

Pristerà et al. 10.1073/pnas.1503911112

SI Materials and Methods

Pharmacological Treatments. Cre-mediated recombination of Foxa1/2 alleles was achieved by intraperitoneal injections of tamoxifen at 8 weeks of age. Tamoxifen (Sigma) was reconstituted in 10% ethanol/90% corn oil (Sigma) at a concentration of 10 mg/mL and kept refrigerated and protected from light. Mice were injected with 1 mg of tamoxifen twice a day, for 5 consecutive days. L-DOPA (Sigma) was prepared in 0.25% ascorbic acid/PBS at a final concentration of 2.5 mg/mL, filtered sterile, and protected from light. L-DOPA and vehicle (0.25% ascorbic acid/PBS) injections were performed twice a day at a dose of 50 mg/kg, for 3 consecutive weeks.

Image Analysis and Quantification. For the quantification of fluorescent intensity and cell counts, images were acquired in structured illumination mode to achieve optical sectioning. Signal intensity of cytoplasmic TH levels in the cell bodies was quantified by Fiji image processing package. Only mDA neurons showing the nucleus in the optic sections were included in the analysis (over 800 neurons analyzed per genotype, from at least four pictures per group), and background fluorescence values were subtracted from all of the readings. For YFP cell counts, the total number of ventral midbrain YFP cells in the SNc and VTA of control and *Foxa1/2* cKO mice were counted on matching coronal sections along the rostrocaudal axis (over 1,800 neurons were counted per genotype, from at least four pictures per group; $n = 3$ per genotype).

rt-qPCR Primers. The following primer sequences were used: Th, forward, 5-CAGAGTTGGATAAGTGTCACCAC-3, and Th, reverse, 5-GGGTAGCATAGAGGCCCTTCA-3; Ddc, forward, 5-CATTCTTGGGTTGGTCTGCT-3, and Ddc, reverse, 5-TTGGCGCTGTTTATTCTTTG-3; Slc18a2, forward, 5-ATGCTATCGGTCCCTCTGCTGGTG-3, and Slc18a2, reverse, 5-GACGGGGTACGGCTGGACATTATT-3; Slc6a3, forward, 5-ATCAACCCACCGCAGACACCAGT-3, and Slc6a3, reverse, 5-GGCATCCCGGCAATAACCAT-3; Drd2, forward, 5-GCCGAGTTACTGTCATGATC-3, and Drd2, reverse, 5-ACGGTGCAGAGTTTCATGTC-3; Fos, forward, 5-CGGGTTTCAACGCCGACTA-3, and Fos, reverse, 5-TTGGCACTAGAGACGGACAGA-3; Gapdh, forward, 5-AAGCCCATCACCATCTTCCA-3, and Gapdh, reverse, 5-GGCAGTGATGGCATGGACTG-3.

Protein Extraction and Western Blotting. Mice were culled, and the midbrain region was rapidly dissected. Tissue was homogenized in ice-cold RIPA buffer (Sigma) supplemented with protease inhibitors (Sigma and Roche) with mortar and pestle on ice. Tissue homogenate was incubated 30 min at 4 °C, while rotating. Following incubation, the sample was passed 10 times through a 23-gauge needle, and insoluble material was spun down for 20 min at 4 °C at 16,000× *g*. Protein concentration of the soluble fraction was quantified by BCA method and 25 μg of total protein was separated by SDS/PAGE. Proteins were transferred onto a PVDF membrane (Bio-Rad) and blocked with 50% (vol/vol) Odissey blocking buffer (Li-Cor) in PBS for 1 h at room temperature. Membrane was subsequently incubated with rabbit anti-TH (1:1,000; Pel-Freez), rabbit anti-pSer40 TH (1:1,000; Millipore), goat anti-FOXA1/2 (1:1,000; Santa Cruz), and mouse anti–α-TUBULIN (1:10,000; Sigma) diluted in 50% Odissey blocking buffer. After several washes, the membranes were incubated for 1 h at room temperature with appropriate secondary antibodies (1:10,000; Li-Cor), conjugated to infrared dyes (IRDye; 700 and 800 nm) or HRP enzyme (1:10,000; Dako). Following extensive washes, membranes were imaged on the Odyssey Infrared Imaging system, or the signal was developed with ECL. TH, pSer40 TH, and FOXA1/2 protein amount, normalized to endogenous α-TUBULIN content, was calculated by measuring signal intensity with Fiji image-processing package.

In Vivo Electrophysiology. All experiments and subsequent analyses were performed blind to genotype. Anesthesia was induced with isoflurane (Isoflo; Shering-Plough) and maintained with urethane (1.5 g/kg, i.p.; ethyl carbamate; Sigma-Aldrich). Anesthesia was monitored during experiments using the electrocorticogram (ECoG) (see below) and by testing reflexes to a cutaneous pinch or gentle corneal stimulation. Corneal dehydration was prevented with application of Hypromellose eye drops (Norton Pharmaceuticals) and eye ointment (Lacri-Lube; Allergan). Protocols for electrophysiology were similar to those previously described (83): Animals were placed in a stereotaxic frame (Kopf), and their body temperature maintained at 37 ± 0.5 °C using a homeothermic heating device (Harvard Apparatus). For ECoG recordings, a stainless-steel screw was implanted above the right frontal cortex (anteroposterior and mediolateral, 2 mm distance from bregma) (82) and was referenced against a screw positioned above the cerebellum. The raw ECoG was bandpass filtered (0.3–1,500 Hz, −3-dB limits) and amplified (2,000×; DPA-2FS filter/amplifier; npi) before acquisition.

A craniotomy was performed above the right and/or left SNc. Saline [0.9% (wt/vol) NaCl] was frequently applied around the craniotomy to prevent dehydration of the exposed cortex. Extracellular recordings of single-unit activity were made with glass electrodes (tip diameter, ∼1.5 μm; in situ resistance, 10–25 MΩ) filled with 0.5 M NaCl containing Neurobiotin [1.5% (wt/vol); Vector Laboratories]. Electrode signals were amplified (10×) through the active bridge circuitry of an Axoprobe-1A amplifier (Molecular Devices). Single units were recorded after alternating current coupling, amplification (100×; DPA-2FS; npi), and standard bandpass filtering (between 300 and 5,000 Hz; DPA-2FS; npi). A Humbug (Quest Scientific) was used to eliminate mains noise at 50 Hz. To avoid possible sampling bias, generous online criteria were applied to guide recordings (spike duration threshold-to-trough for bandpass-filtered spikes of >0.8 ms and firing rates <20 Hz) (83).

Following the recording, single neurons were labeled with Neurobiotin using the juxtacellular method (84) to allow for their unambiguous identification and localization. In brief, the electrode was advanced slowly toward the neuron while a microiontophoretic current was applied (1- to 10-nA positive current, 200-ms duration, 50% duty cycle). The optimal position of the electrode was identified when the firing pattern of the neuron was robustly modulated by the current injection. The Neurobiotin was then left to transport along neuronal processes for up to 12 h. At the end of the experiment, animals were given a lethal dose of anesthetic and transcardially perfused with 20 mL of 0.01 M PBS at pH 7.4 followed by 40 mL of 4% (wt/vol) PFA in 0.1 M phosphate buffer, pH 7.4. Brains were left in PFA at 4 °C until they were sectioned 12–72 h later.

All biopotentials were digitized online using a Power 1401 analog-digital converter (Cambridge Electronic Design) and acquired using Spike2 software (version 7.12; Cambridge Electronic Design). Only unit activity recorded during robust cortical slow-wave activity (SWA) was included in the analysis. For the extraction of SWA periods, electrocorticogram data were Fourier-transformed (frequency resolution, 0.2 Hz), and the

power ratio in the SWA band (0.5–2 Hz) to the power in the gamma band (30–80 Hz) was calculated. Epochs of contiguous data with a power of >13 for each data point were concatenated for further analysis. Putative single-unit activity was isolated using template matching, principal component analysis, and supervised clustering within Spike2. Firing variability was calculated using CV2 (85), which compares the variability of adjacent interspike intervals (ISIs) within a spike train, and then a mean CV2 value was obtained for each neuron (lower CV2 values indicate more regular unit activity). Bursts in DAergic SNc neurons were determined using the Robust Gaussian Surprise (RGS) method (86), a statistical method to detect clusters of spikes with significantly lower ISIs than a central distribution obtained from the pooled and normalized spike trains. Percentage of total numbers of spikes emitted in bursts was calculated from RGS obtained clusters. RGS parameters were set to a minimum of two spikes per burst. For the classification of in vivo firing patterns, autocorrelation histograms (ACHs) of each individual neuron were plotted (5-ms bins, 2-s window). Each ACH was classified by visual inspection as one of three modes: regular (≥3 equally spaced peaks), irregular (less than three peaks increasing from zero approximating a steady state), or bursty (narrow peak with increase at short ISIs) (87). Classifications were then used to ascribe a firing mode to individual cells within each genotype.

Fast-Scan Cyclic Voltammetry. Pairs of 3-months-old control and adult *Foxa1/2* cKO male mice, 25–39 d posttamoxifen, were killed by cervical dislocation and decapitated. Coronal slices (300 μm) containing the striatum were prepared as described previously in ice-cold Hepes-buffered artificial cerebrospinal fluid (aCSF) saturated with 95% O_2/5% CO_2. Slices were then maintained in a bicarbonate-buffered aCSF at room temperature before recording. Extracellular DA concentration ($[DA]_o$) was monitored using fast-scan cyclic voltammetry (FCV) with 7-μm-diameter carbon fiber microelectrodes (tip length, 50–100 μm) and a Millar voltammeter (Julian Millar, Barts and the London School of Medicine and Dentistry, London, UK) as described previously (83). In brief, the scanning voltage was a triangular waveform (−0.7- to +1.3-V range vs. Ag/AgCl) at a scan rate of 800 V/s and sampling frequency of 8 Hz. The two genotypes being compared on a given recording day were age-, sex-, and days posttamoxifen-matched. Electrodes were calibrated in 2 μM DA.

HPLC with Electrochemical Detection. DA content was measured by HPLC with electrochemical detection as previously described (83). DA content was assessed both in forebrain chunks and in tissue punches from slices following FCV recordings in dorsal and ventral striatum. Forebrains were extracted following cervical dislocation and decapitation, weighed, and snap frozen on dry ice in 750 μL of 0.1 M $HClO_4$. Following FCV recordings, tissue punches from the dorsal (2 mm diameter) and ventral striatum (1.2 mm diameter) from two brain slices per animal were taken and stored at −80 °C in 200 μL of 0.1 M $HClO_4$. On the day of analysis, samples were thawed, homogenized, and centrifuged at 16,000 × *g* for 15 min at 4 °C. The supernatant was analyzed for DA content using HPLC with electrochemical detection. Analytes were separated using a 4.6 × 250-mm Microsorb C18 reverse-phase column (Varian or Agilent) and detected using a Decade II SDS electrochemical detector with a Glassy carbon working electrode (Antec Leyden) set at +0.7 V with respect to a Ag/AgCl reference electrode. The mobile phase consisted of 13% methanol (vol/vol), 0.12 M NaH_2PO_4, 0.5–2.0 mM OSA, and 0.8 mM EDTA, pH 3.5–4.6, and the flow rate was fixed at 1 mL/min. Analyte measurements were normalized to tissue punch volume (in picomoles per cubic millimeter), or tissue chunk weight (in picomoles per milligram). All data are expressed as means ± SEM; the sample size, *n*, is the number of observations; and *N* is the number of animals. Comparisons for differences in means were assessed by two-way ANOVA followed by post hoc Bonferroni's *t* test or unpaired *t* tests using GraphPad Prism 6.0 (GraphPad Software).

Behavior. Male mice were individually housed 1 week before testing in Tecniplast cages (32 × 16 × 14 cm) with sawdust, a cardboard shelter, and additional bedding material with ad libitum access to water and food. Cages were changed once every 2 weeks but never on the day before, or the day of, testing to minimize the disruptive effect of cage cleaning on behavior. The housing room was maintained at constant room temperature (21 °C) and humidity (45%) and kept under a regular light/dark schedule with lights on from 0800 to 2000 h (light = 270 lx).

Tests were carried out in the following order: home cage, sucrose preference, rotarod, and grip strength. After each test, boli and urine were removed from the test arena, which was then cleaned with 1% Trigene solution. All behavioral tests were performed in the light phase between 0900 and 1800 h, except for the home cage. Experimenters were blind to the genotypes of the animals both during testing and subsequent scoring of the recorded behavior. The mice were regenotyped following behavioral testing to confirm genotype.

For home cage activity, spontaneous locomotion was recorded in their home cage at three different time points during the dark phase (1 h after lights off, 1 h in the middle of the dark phase, and 1 h before lights on), across a single 24-h time period (88). Red cluster lights (LED cluster red light no. 310-6.757; RS Components) of approximate wavelength 705 nm provided minimal red light for video recording during the dark phase. Home cage activity was recorded using an overhead camera and subsequently tracked using Ethovision software (version 3.1; Noldus Information Technology). Parameters extracted and analyzed included distance traveled (in meters) and the number of visits to the feeding/drinking area.

Anhedonia was measured using the sucrose preference task (89). Mice were habituated to a two bottles paradigm in their home cage over 24 h with both bottles containing water. Twenty-four hours later, mice were given a free choice between two bottles, one with 2% (wt/vol) sucrose solution and another with tap water for 48 h. (The location of the sucrose and water bottles was switched after 24 h to avoid any location preference.) Extra care was taken to avoid liquid spillage, and bottles were filled in advance and kept overnight in the housing room to reduce any effects of the room temperature and pressure on the bottles. The intake of water and 2% sucrose solution and total intake was estimated by weighing the bottles before and after the test session, every 24 h. The preference for sucrose was calculated as the percentage of the sucrose solution consumed out of the total amount of liquid consumed (sucrose solution intake/total intake × 100).

Motor learning, coordination, and balance were assessed using a Rota-Rod 47600 testing device (Ugo Basile). Mice were tested as described by Holmes et al. (90). Mice were tested for 2 consecutive days, three times a day. Mice were placed on an accelerating rotarod (0–40 rpm over 5 min) and latency to fall was recorded, with increasing latencies indicative of better performance in the task.

A Linton grip strength meter (MJS Technology) was used to measured forelimb and hindlimb grip strength as an indicator of neuromuscular function as previously described (91). The grip strength meter was positioned horizontally, and mice were held by the tail and lowered toward the apparatus. Mice were allowed to grasp the metal grid with their forelimbs and were then pulled backward in the horizontal plane. The force in grams applied to the bar at the moment the grasp is released was recorded by the machine as their grip strength. This was repeated three times, and the average grip strength for each mouse was calculated. The same was repeated for the hindlimbs. Mice were not trained before testing.

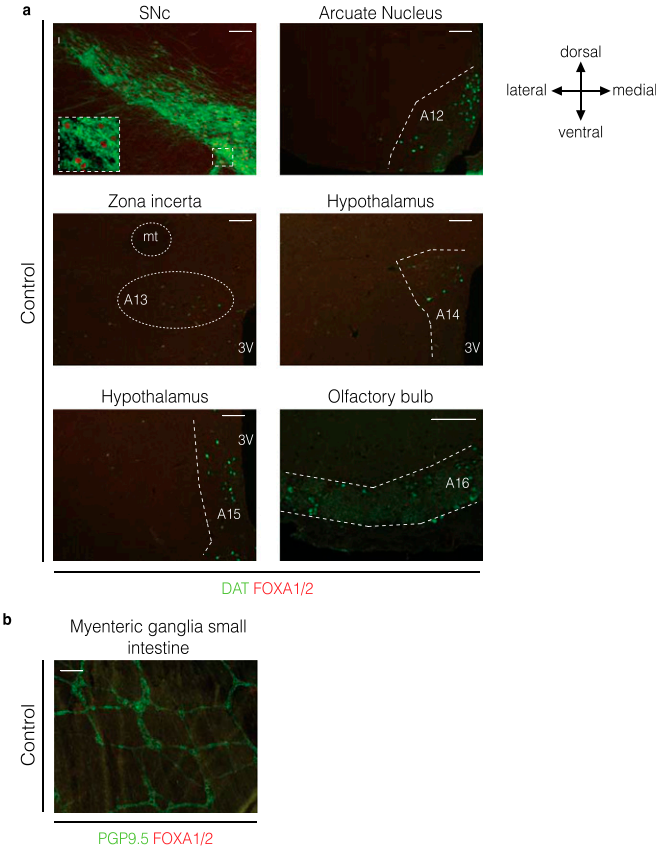

Fig. S1. FOXA1/2 are expressed in adult mDA neurons but not in the DAergic neurons of the hypothalamus and in the enteric nervous system. Images show FOXA1/2 immunoreactivity in DAT-expressing mDA neurons (SNc) of control mice, and their absence in DAT-expressing neurons of the arcuate nucleus (A12), of the zona incerta (A13), of the hypothalamus (A14–A15), and of the olfactory bulbs (A16) (*A*). Image in *B* shows absence of FOXA1/2 immunoreactivity in neurons of the enteric nervous system, identified by PGP9.5 expression. mt, mammillothalamic tract; 3V, third ventricle. (Scale bars: 100 μm.)

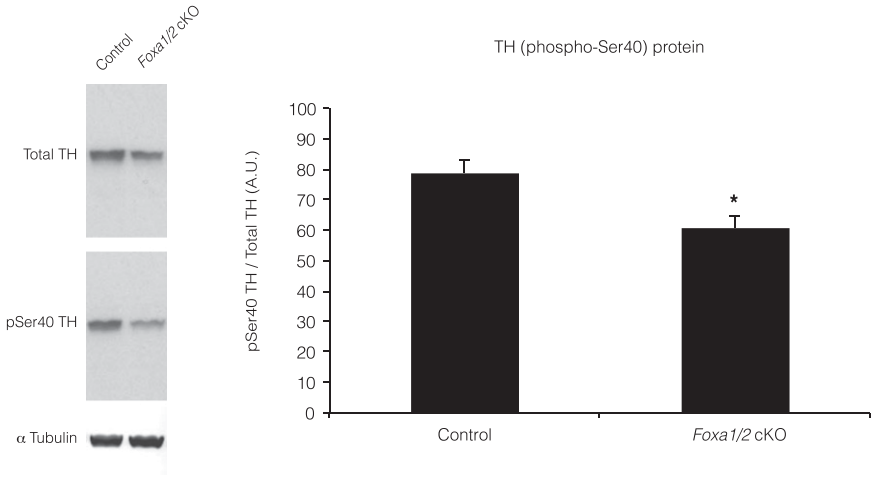

Fig. S2. Adult *Foxa1/2* cKO mice show reduced pSer40 TH levels compared with control mice. pSer40 TH protein levels were quantified by Western blotting, and a representative blot for total TH, pSer40 TH, and α-TUBULIN, used as loading control, are shown. Bar graph, obtained by densitometric analysis of Western blot data, shows pSer40 TH protein amount in adult control and *Foxa1/2* cKO mice. Values represent density of pSer40 TH bands normalized to total TH band density, and are expressed as mean ± SEM [pSer40 TH protein amount in adult control mice, 78.7 ± 4.2 (A.U.); pSer40 TH protein amount in adult *Foxa1/2* cKO, 60.6 ± 4.2 (A.U.), $n = 4$; $^*P < 0.05$ vs. control, *t* test].

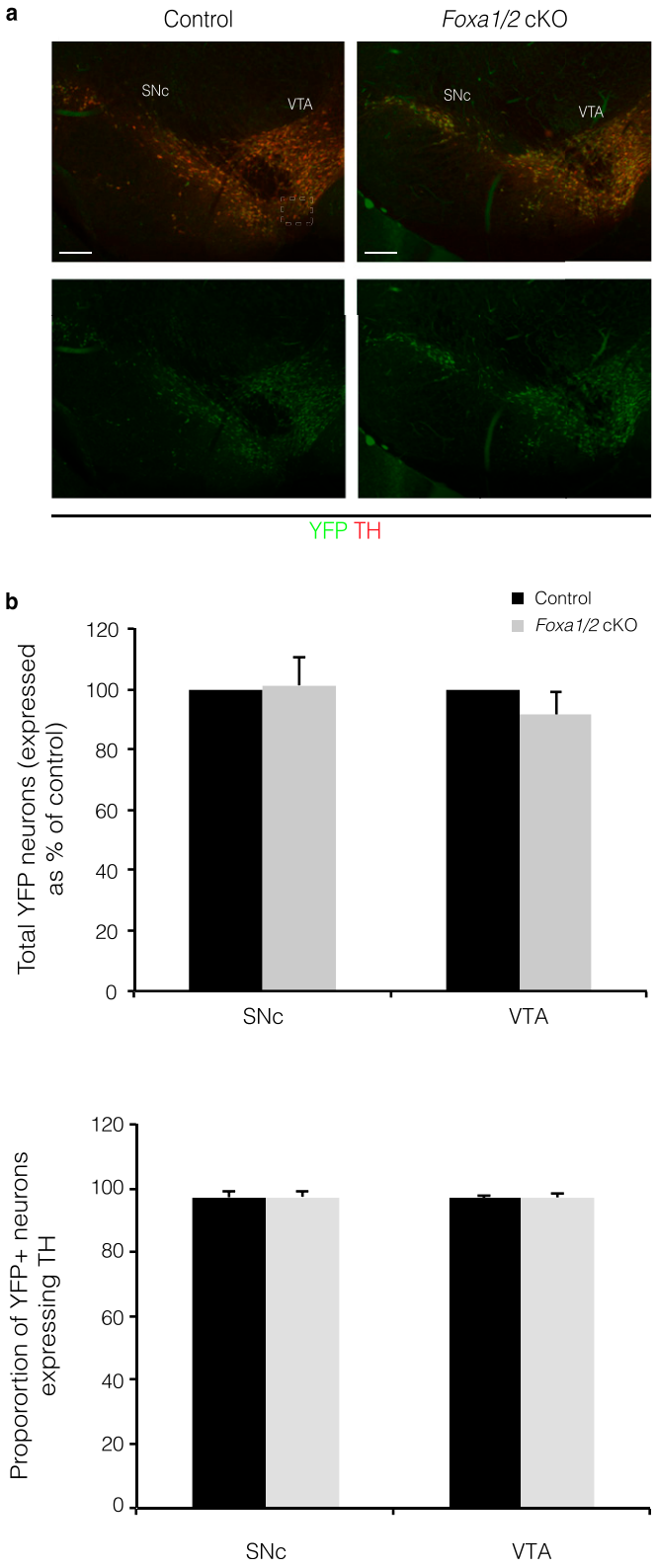

Fig. S3. Absence of FOXA1/2 does not lead to neuronal cell loss. Images show representative YFP and TH immunoreactivity in mDA neurons of control and adult *Foxa1/2* cKO mice, 4 weeks after tamoxifen-mediated recombination. The bottom panel shows YFP only immunoreactivity for clarity purposes. [Scale bars: 200 μm (*A*).] Graphs show the total number of YFP neurons (*Top*) and the proportion of YFP positive neurons expressing TH (*Bottom*) in the SNc and VTA of control and *Foxa1/2* cKO mice (*B*) ($n = 3$; mean ± SEM, *t* test, *Foxa1/2* cKO vs. control not significant).

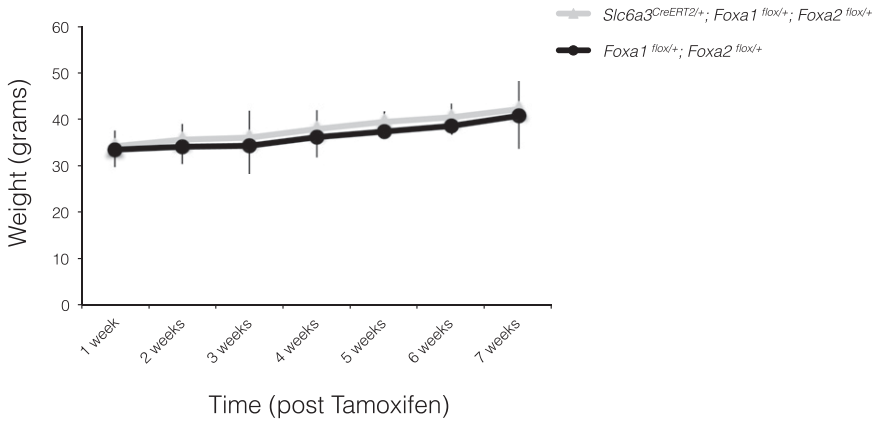

Fig. S4. Tamoxifen injections in adult mice heterozygous for FOXA1 and FOXA2 at 8 weeks of age does not lead to weight loss. Graph shows body weight in grams, recorded weekly after tamoxifen injections. Each data point represents mean ± SEM (*Slc6a3*$^{CreERT2/+}$;*Foxa1*$^{flox/+}$;*Foxa2*$^{flox/+}$, $n = 9$; *Foxa1*$^{flox/+}$;*Foxa2*$^{flox/+}$, $n = 4$).

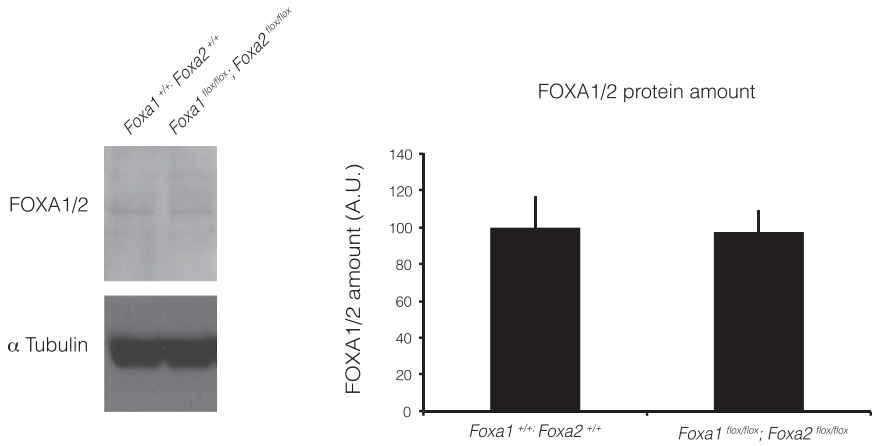

Fig. S5. FOXA1/2 protein levels are similar in mDA neurons of adult wild-type and *Foxa1*$^{flox/flox}$;*Foxa2*$^{flox/flox}$ mice. Total proteins were extracted from ventral midbrain tissue and FOXA1/2 protein levels were quantified by Western blotting. A representative blot for FOXA1/2 and α-TUBULIN, used as loading control, is shown. Bar graph, obtained by densitometric analysis of Western blot data, shows FOXA1/2 protein amount in *Foxa1*$^{flox/flox}$;*Foxa2*$^{flox/flox}$ mice compared with mice bearing wild-type alleles. Data are expressed as percentage change of FOXA1/2 levels in *Foxa1*$^{flox/flox}$;*Foxa2*$^{flox/flox}$ vs. wild-type mice (graph) ($n = 3$; mean ± SEM, *t* test, *Foxa1*$^{flox/flox}$;*Foxa2*$^{flox/flox}$ vs. wild type, $P = 0.91$).